

---

# INDUCTIVE BIASES IN DEEP LEARNING MODELS FOR WEATHER PREDICTION

---

A PREPRINT

<b>Jannik Thuemmel*</b> Machine Learning in Climate Science University of Tübingen, Germany	<b>Matthias Karlbauer</b> Neuro-Cognitive Modeling University of Tübingen, Germany	<b>Sebastian Otte</b> Neuro-Cognitive Modeling University of Tübingen, Germany
<b>Christiane Zarfl</b> Environmental Systems Analysis University of Tübingen, Germany	<b>Georg Martius</b> Autonomous Learning Max Planck Institute for Intelligent Systems Tübingen, Germany	
<b>Nicole Ludwig</b> Machine Learning in Sustainable Energy Systems University of Tübingen, Germany	<b>Thomas Scholten</b> Soil Science and Geomorphology University of Tübingen, Germany	
<b>Ulrich Friedrich</b> Research and Development Deutscher Wetterdienst, Offenbach, Germany	<b>Volker Wulfmeyer</b> Institute of Physics and Meteorology University of Hohenheim, Stuttgart, Germany	
<b>Bedartha Goswami</b> Machine Learning in Climate Science University of Tübingen, Germany	<b>Martin V. Butz</b> Neuro-Cognitive Modeling University of Tübingen, Germany	

## ABSTRACT

Deep learning has recently gained immense popularity in the Earth sciences as it enables us to formulate purely data-driven models of complex Earth system processes. Deep learning-based weather prediction (DLWP) models have made significant progress in the last few years, achieving forecast skills comparable to established numerical weather prediction (NWP) models with comparatively lesser computational costs. In order to train accurate, reliable, and tractable DLWP models with several millions of parameters, the model design needs to incorporate suitable inductive biases that encode structural assumptions about the data and modelled processes. When chosen appropriately, these biases enable faster learning and better generalisation to unseen data. Although inductive biases play a crucial role in successful DLWP models, they are often not stated explicitly and how they contribute to model performance remains unclear. Here, we review and analyse the inductive biases of six state-of-the-art DLWP models, involving a deeper look at five key design elements: input data, forecasting objective, loss components, layered design of the deep learning architectures, and optimisation methods. We show how the design choices made in each of the five design elements relate to structural assumptions. Given recent developments in the broader DL community, we anticipate that the future of DLWP will likely see a wider use of foundation models—large models pre-trained on big databases with self-supervised learning—combined with explicit physics-informed inductive biases that allow the models to provide competitive forecasts even at the more challenging subseasonal-to-seasonal scales.

---

\*Correspondence to: [jannik.thuemmel@uni-tuebingen.de](mailto:jannik.thuemmel@uni-tuebingen.de)

## 1 Introduction

Accurate weather forecasts play an important role in different aspects of modern society including agriculture, infrastructure, transportation, aviation, and disaster mitigation. Ongoing climate change in particular increases the likelihood of extreme weather patterns on all scales [1, 2]. This creates the immediate demand for new models that can cope with these more erratic and extreme weather patterns in order to provide reliable forecasts for the public welfare in the next decades. Until now, operational weather forecast models, which regularly issue predictions from minutes to days to weeks, rely on numerical weather predictions (NWP, [Box 1](#)). NWP models are constructed by experts from physics, geoscience, and meteorology as well as from data analysis, statistics, and computer science to perform well.

Over the past three decades, NWP models have made significant improvements in providing highly accurate weather forecasts, particularly up to weekly timescales. For instance, forecast skills, which quantify improvements made over a baseline, for a 5-day forecast increased from slightly over 70% in the mid-nineties to over 90% in 2015 (cf. Figure 1 in [3]). Termed the ‘quiet revolution’ because of its incremental nature, the progress in NWP was made possible mainly by improvements in modelling subgrid processes, data assimilation and resulting model initialisation, and ensemble prediction ([Box 1](#)). The gains in these areas crucially depended on concomitant advancements in computational technologies such as the availability of faster and more efficient computing chips, which has in recent years shown signs of slowing down, and has sparked new discussions of how NWP models can be adapted to the road ahead [4].

Purely data-driven weather forecast models powered by deep learning (DL, [Box 2](#)) are on the verge of triggering a major breakthrough in weather forecasting. An early study in this direction used convolutional Long Short Term Memory (LSTM) networks for precipitation nowcasting [5]. Early attempts to model global atmospheric states include a multilayer perceptron [6] and a convolutional neural network (CNN) architecture (with an LSTM variant) to forecast mid-tropospheric geopotential height [7], as well as an autoencoder setup to forecast the weather within a simple climate model [8]. Many similar studies that followed over the last four years have demonstrated the potential of using deep learning models for weather prediction (DLWPs).

One fundamental reason why it is attractive to think of using DL for predicting the weather is its apparent simplicity—we do not need to fully understand nor explicitly model the physics of the atmosphere as thoroughly as in NWPs. NWP models themselves are highly complicated objects with many interdependent handcrafted modules and tuning parameters, which make them hard to adapt to new situations. In contrast, DLWPs may self-organise and learn the necessary abstract representations of atmospheric dynamics required to predict the weather accurately at scale, and infer the influences of subgrid processes and interactions between them while doing so ([Box 2](#)). The fact that DL requires less modelling effort and imposes less representational constraints forms the basis for using it to solve complex problems. The self-organising nature of DL enables faster model design and more flexible inferences of complex correlation patterns as long as sufficient amounts of data are available [9]. Moreover, once a DLWP model has been trained, the forward inference of a forecast can be conducted at a fraction of the energy and time investment of an NWP forecast [10], which may support larger ensembles and more accurate uncertainty quantification.

We are also currently in an age where weather prediction models have access to high resolution meteorological data sources. The ERA5 dataset, for instance, offers global atmospheric reanalysis data on 37 pressure levels with a spatial resolution as high as  $0.25^\circ \times 0.25^\circ$  [11]. For DLWP models, the WeatherBench benchmark [12] catalysed model development by facilitating the intercomparison of new models against the state-of-the-art. Deep learning has by now made significant gains in modelling atmospheric dynamics via both purely DLWP models and hybrid DLWP-NWP models [13–16]. Pure DLWP models in particular have shown impressive performance in precipitation nowcasting and are competitive with state-of-the-art forecast methods [17, 18]. In some cases, DLWP forecasts of global mid-term weather dynamics have also been shown to outperform NWP model forecasts [19, 20]. Even on the sub-seasonal to seasonal timescales, first skilful forecasting results have been reported recently [21].

When setting up a DL model, design choices are necessary, which induce implicit and nontrivial inductive learning and information processing biases. Inductive biases (c.f. [Box 2](#)) essentially implement prior assumptions about the modelled system dynamics, aiming at both keeping the learning problem tractable and fostering generalisation [22]. In order to develop a DLWP model that is tractable, generalisable to out-of-data scenarios, and explainable, the inductive biases ([Box 2](#)) in the DLWP model need to be well-chosen.

This review focuses on the inductive biases of six high-performing, state-of-the-art DLWP models for short- to mid-range weather forecasting:

- Ravuri et al (R21 [18]) implement a generative model for nowcasting precipitation up to 90 minutes into the future with highly realistic trajectories.
- Espeholt et al (E21 [17]) make probabilistic forecasts of precipitation for up to twelve hours and rival the forecast skill of physical methods.

**Box 1. Numerical Weather Prediction**

Numerical Weather Prediction (NWP) primarily combines Navier-Stokes equations governing fluid dynamics with principles of mass and momentum conservation, the idealised gas law, and the first law of thermodynamics [27]. The result is a system of nonlinear, partial differential equations that model the physical processes unfolding in the atmosphere. To generate weather forecasts, given initial conditions that accurately describe the state of the atmosphere, the set of equations are numerically integrated in time on discretised, three-dimensional grid structures. State-of-the-art operational NWP models cover a wide range of spatial and temporal forecast scales: from local, sub-hourly kilometre-scales, to mid-term, weekly-scales, to global seasonal scales. In all cases, though, inherent nonlinearities of atmospheric dynamics impose a hard limit on how far ahead in time we can predict the weather. Variations in performance of different NWP models depend on various design choices, of which the two most relevant aspects are how subgrid processes are modelled and how the data is assimilated.

**Subgrid physical processes.** Regardless of the NWP's spatial and temporal resolution, physical processes below the model resolution will influence the modelled dynamics. These unresolved processes impact model evolution mainly via its thermodynamics (energy transfer) and dynamics (momentum transfer). Typically, such processes are included in the NWP via approximations known as 'parameterisations', which heuristically quantify their interaction with the properly resolved physical processes. Better model parameterisations form a central objective of current NWP research [28]. Typical subgrid processes include the formation of clouds, deep convection, and land-atmosphere interactions. Accurate parameterisations have a strong impact on the predictive power of NWPs as they influence crucial model variables such as precipitation, temperature, and wind [29].

**Ensemble modelling** Inherent nonlinearities of atmospheric dynamics impose a hard limit on how far ahead in time we can predict the weather. A small error in specifying the initial atmospheric state can result in a predicted state that is drastically different from what is observed [30]. Probabilistic weather forecasts based on an ensemble of initial conditions, combined with online data assimilation try to tackle the problem by sampling the possible states in the future as best as possible with a given set of initial conditions, and then integrating the model with only those trajectories that are the most probable, given the latest observations [31]. This results in a forecast cycle, which goes from initial conditions to a first ensemble estimate, followed by a re-initialisation based on data assimilation, a second, more constrained ensemble, and so on. Strategies for model initialisation, data assimilation, and ensemble analysis crucially influence the predictive skill of NWP models.

- Weyn et al (W21 [23]) forecast global weather with highly domain-driven design choices, featuring the generation of plausible dynamic even on sub-seasonal scales.
- Pathak et al (P22 [24]) utilise very high spatial resolutions to forecast global weather, emphasising the prediction of impactful surface variables and extremes.
- Keisler (K22 [25]) implements a graph neural network with promising results on mid-range global weather forecasting.
- Hu et al (H22 [26]) further show the potential of generative models to produce skilful DLWP ensemble forecasts for global weather.

The six covered DLWPs indicate a wide range of neural architectures and DL techniques that have been used to successfully forecast the weather on various spatial and temporal scales and with different input and target variables. Our review highlights the design choices made in the six models and discusses the impacts of other potential design options. We thus aim to conceptualise the six models and the applied techniques therein to foster our understanding of DLWP in general and to facilitate application and further development of DLWPs.

## 2 Key design elements

In order to identify and characterise distinct inductive biases (c.f. **Box 2**) in the current best-performing DLWPs, it is useful to conceptualise DL architectures by means of the following five design elements:

- **Data selection**, including the choice of variables and forecast scales, forms the basis for all other design choices.
- **Learning objectives** outline the functionality of the model by defining the forecast target and, potentially, how to handle uncertainty.
- The **loss function** quantifies how well the model predictions fit the data and enables gradient-based optimisation.

**Box 2. Deep Learning**

Deep learning (DL) refers to artificial neural networks that contain many layers, thus transforming input data via abstract, compositional, and hierarchical representations into target predictions [9, 32]. Each layer in a neural network architecture consists of computational units called neurons, which receive information from other layers, combine this information, for example, via a weighted sum, and produce a consequent output with a typically non-linear but differentiable activation function. During training, the weights self-organise via error backpropagation such that the neurons and layers encode latent features for minimising a pre-specified, task-specific performance criterion. Training is complete when no further performance gain is made or when over-fitting is registered, which is the case when performance starts stalling or even declining on an evaluation set while it is still improving on the training set. The trained model can then be used with its learned set of weights to generate predictions about new data instances.

**Latent representations.** Observable data spaces are often inadequate to predict future system states efficiently. This happens because crucial system dynamics are warped in the data dimensions, take place on a manifold of smaller dimensionality, or are controlled by structures and patterns that are not directly accessible in data space. Thus, transforming the data to identify the latent structure that properly describes the dynamics of the system is an important goal. DL excels in the self-organisation of data projections into latent spaces, learning representations that are better-suited for the effective generation of accurate predictions [33].

**Inductive bias.** Problem-targeted learning in DL is accomplished by implementing well-motivated structural assumptions about the data and the modelled processes [34, 35], known as inductive biases [22]. Inductive biases can accelerate model convergence and can improve both computational efficiency and generalisation to unseen data. For example, a convolutional DL model induces the bias that pixels close to each other contain correlated information, thus excelling at classifying images when compared to a standard artificial network (multilayer perceptron), which does not inform about spatial proximity. In principle, any design choice (e.g., data normalisation, pre-training, number and type of layers, and optimisation criteria) incorporates implicit inductive biases, which influence model generalisability and performance. To design reliable DL models, it is thus crucial to be aware of the incorporated inductive biases.

- The **neural network architecture** distinctively encodes the data, processes system dynamics, and finally decodes consequent forecasts.
- **Optimisation** of DLWP model parameters by means of a particular training scheme determines the model adaptation process.

Following this design choice partitioning, we introduce key DL concepts, provide background references, and highlight the implemented design choices in the six considered DLWP models. We particularly focus on the respectively induced inductive biases.

## 2.1 Data selection

Data selection is critical to enable DLWP models to make accurate predictions and highly depends on the targeted prediction task. In application, availability of high quality data and sufficient computational resources also influences the data selection. As a result, the considered DLWP differ substantially in their data choices, an overview of these choices is shown in [Table 1](#).

### 2.1.1 Precipitation nowcasting

Nowcasting of precipitation refers to prediction tasks in the immediate future ranging from a few minutes up to several hours, with the exact definition varying between operational weather centres. Both R21 and E21 predict precipitation up to 90 minutes or up to 12 hours, respectively.

Within the nowcast timescale, short-lived high impact precipitation events are of particular interest. Such events may lead to flash floods, include hail events and may shut down airports. Especially intense rainfall, e.g., during a thunderstorm, can be sharply localised and brief [36]. To resolve precipitation, the data is thus required to satisfy high resolution both in space and time, such as a 1 km or lower scale sampled on 1 to 15 minute intervals. Radar stations measure the reflectivity of water droplets in the air [37, 38]. Geostationary weather satellites [39, 40] sense outgoing radiation across multiple wavelengths, to, e.g., measure the presence and thickness of clouds and the release of heat during convection, which is an essential ingredient for thunderstorm formation. Ground-based rain gauges measure the accumulated precipitation at their location. In R21, precipitation is estimated from radar measurements with a 5 minute interval and a 1 km spatial resolution. E21 predict both, instantaneous precipitation as estimated from radar

Table 1: Data selection across considered DLWP models. The choice of **variables** defines the information the model has access to. Prescribed fields do not depend on model outputs but are known in advance (e.g. orography, assimilation variables). The prognostic surface and atmospheric variables are the main forecasting targets. The ‘13 levels’ are the pressure levels defined in WeatherBench [12], i.e., 50, 100, 150, 200, 250, 300, 400, 500, 600, 700, 850, 925, and 1000 hPa. The **forecast resolution** has strong implications for the computational complexity of the learning problem, as well as for the complexity and types of physical processes that can be modeled. The first and second entry in the cells of the ‘horizontal’ column refer to data resolution and forecast area, respectively.

Variables			Forecast resolution		
Prescribed	Near-surface	Atmospheric	Vertical	Horizontal	Temporal
<b>R21</b>	None	Precipitation	None	None	1 km 256 km 5 min < 90 min
<b>E21</b>	Geospatial coordinates Satellite observations Assimilation variables (NWP forecast)	Precipitation	None	None	1 km 512 km 2 min < 12 h
<b>W21</b>	Orography Land-sea mask Incident solar radiation	2 m temperature	Temperature Geopotential Total column water vapor Geopotential thickness	850 hPa 500, 1000 hPa Integrated 300 – 700 hPa	1.4 ° Global 6 h
<b>P22</b>	None	2 m temperature 10 m $U, V$ winds Surface pressure Sea-level pressure (Total precipitation)	Temperature Geopotential Relative humidity $U, V$ winds Total column water vapor	500, 850 hPa 50, 500, 850, 1000 hPa 500, 850 hPa 500, 850, 1000 hPa Integrated	0.25 ° Global 6 h
<b>K22</b>	Geospatial coordinates Orography Land-sea mask Incident solar radiation	None	Temperature Geopotential Specific humidity $U, V, W$ winds	13 levels 13 levels 13 levels 13 levels	1 ° Global 6 h
<b>H22</b>	Orography Land-sea mask	2 m temperature 10 m $U, V$ winds Total precipitation	Temperature Geopotential Relative Humidity $U, V$ winds	13 levels 13 levels 13 levels 13 levels	5.6 ° Global 6 h

measurements with a 2 minute interval and a 1 km spatial resolution, as well as hourly accumulated precipitation which integrates radar and rain gauge measurements.

In practice, nowcasting methods for the immediate future (e.g. minutes to few hours) are often based on optical flow advection schemes. Here, a motion vector field is derived from consecutive data measurements. Typically, this flow information is used to advect the data in a (semi)-lagrangian way to the desired lead-time. Such methods rely on stationary assumptions both in the data values and of the derived flow information. Since this assumption is only an approximation of reality, a probabilistic component is often added to the forecast model, creating a distribution over possible trajectories [41]. In principle, this is the approach taken by R21, who rely on radar reflectivity data only.

Optical flow-based methods are not effective if the targeted forecast horizon extends to several hours, hence further observational data has to be incorporated. For example, the presence of low- or high pressure systems and moisture transport plays an increasingly important role [42]. In E21 a wide range of additional observations (cf. Table 1) are assimilated into the DLWP’s latent state representation. These observations include geospatial coordinates and elevation, satellite imagery at a 15 minute interval, and hourly estimates of 612 oceanic and atmospheric variables like wind, humidity, temperature and pressure at various altitudes with a 3 km spatial resolution, which are obtained from NWP data assimilation schemes.

### 2.1.2 Mid-range forecasts of atmospheric states

The remaining four models (W21, P22, K22, H22) generate global mid-range weather forecasts (up to ten days). On the global scale, atmospheric dynamics evolve as a complex interplay of multiple variables [27], including temperature, pressure (also called geopotential), humidity, and wind fields in three dimensions (U, V, and W for zonal/eastward, meridional/northward, and vertical components, respectively) [43]. Beyond the variables that directly characterise the atmospheric state, it is beneficial to include prescribed boundary condition information. Information sources that act as region-specific system modulators play an important role. For example, geospatial coordinates may enable a model to indirectly account for orographically induced or region-specific dynamics. More explicitly, a land-sea mask and orographic data, typically provided as a digital elevation model, may be used as input data. Top of atmosphere incident solar radiation refers to the amount of radiation from the sun that arrives at the top of the atmosphere. It depends only

on the rotation of the earth and can thus be computed for many years in advance. Accordingly, it is a forcing variable that acts as a proxy for both the day-night- and the seasonal-cycle.

The commonly used source for training data at a global scale is the ERA5 re-analysis dataset [11], or derivatives thereof [12, 44]. Among the reviewed models, ERA5 derived data is used by W21, P22, K22 and H22 at varying resolution (c.f. [Table 1](#)). Re-analysis data is generated by tuning the initial conditions of an NWP model, such that the mismatch between forecasts and observational data is minimised. Observations are gathered from a wide range of measurements, including ground-based weather stations, balloons, and satellites. ERA5 data covers all atmospheric and many auxiliary variables. It spans an hourly time range from 1940 to 2021 on a horizontal resolution of  $0.25^\circ$  and 37 vertical levels, resulting in up to nine peta-bytes of data.

Both horizontal and vertical resolution play an essential role for weather prediction tasks. Latitude and longitude components are typically reported in degree, where  $1^\circ$  corresponds to roughly 100 km at the equator. Vertical resolution is often given in levels of potential height, that is, the altitude above sea level at which the potential energy (pressure) of the air column equals a pre-defined amount [45]. The exact height of these levels varies with humidity, temperature, and other factors [46–48]. Many of these variables can be integrated over a certain range of vertical levels, yielding aggregate descriptions of air columns. This is done prominently by W21 saving substantial computational resources while maintaining critical information about the atmospheric state.

The scales on which the considered variables evolve can differ substantially—a fact that is reflected in the choice of resolution and variables by the models under review (cf. [Table 1](#)). Mid-range forecasts, however, rely far less on fast changing atmospheric processes and can thus model the relevant dynamics with appreciable accuracy even at coarser spatial resolutions, as demonstrated in W21 and previous work [7, 13]. The high spatial resolution used in P22 enables their model to, for the first time in global DLWP, resolve near-surface winds and hurricanes well enough to produce skilful forecasts. K22 and H22 forecast the global atmospheric state across many vertical levels and over various variables and find that the increased vertical resolution leads to substantial performance gains. Although the coarser resolution in H22 poses a challenge to accurately predict wind and precipitation, a stochastic component in H22 likely counteracts the decrease in predictability, as discussed in further detail below. Most recently, the models introduced in [20] and [19] have shown that DLWP models can indeed be successfully trained on very high horizontal and vertical resolutions, exhibiting superior performance compared to coarser resolution approaches.

## 2.2 Learning objectives

The objective defines the functional mapping that the model will represent, e.g., a classifier, a predictor, or a generative model. In the context of DLWP, we discuss objectives which define a (distribution over) future atmospheric state(s) as target. [Figure 1](#) illustrates the objectives of the six considered models. Forecasting objectives depend on the temporal process that is modelled. Here, we follow the common distinction between iterative and direct forecasts (see e.g. [12, 49]). Moreover, we review the challenges involved in generating probabilistic forecasts.

### 2.2.1 Iterative forecasts

Iterative approaches predict a sequence of future states by feeding their own outputs back as input, forming a closed loop. We further distinguish two kinds of iterative objectives: auto-regressive and recurrent models. Autoregressive models only depend on the last time step to generate a prediction, which turns into the only information available in the next step. Recurrent models, which mimic hidden Markov models, maintain an internal state representation that allows for memory effects beyond the last frame. They are generally able to model more complex temporal interactions [50].

Two issues arise with iterative forecasting methods: (i) a mismatch between ground truth and model generated inputs may lead to increasingly divergent predictions, and (ii) temporal patterns that extend beyond the number of steps that are included in the training objective may be fully ignored by the model. Both issues can be addressed by training the model not only on one-step-ahead predictions, but on longer closed-loop predictions, where the model is forced to deal with its own inputs and subsequent errors [51, 52]. However, each additional prediction step linearly increases the computational complexity of the optimisation and inference procedure, necessitating a trade-off between temporal representation and time complexity. To achieve ideal trade-offs, curriculum learning strategies (cf. [Section 2.5](#)) may be applied to dynamically adapt the objective throughout the optimisation procedure. Increasing the forecast horizon can also lead to optimisation difficulties in the form of vanishing or exploding gradients: Model errors may be amplified or suppressed with each subsequent iteration step [53, 54]. To counteract vanishing gradients, recurrent methods often utilise a gating mechanism [55] that supports gradient flow across time and induces a natural invariance to (small) changes in the time scale [56]. Exploding gradients, on the other hand, have to be addressed by carefully choosing an appropriate forecast time scale, learning rate, and regularisation; especially when the dynamics are chaotic [57, 58].

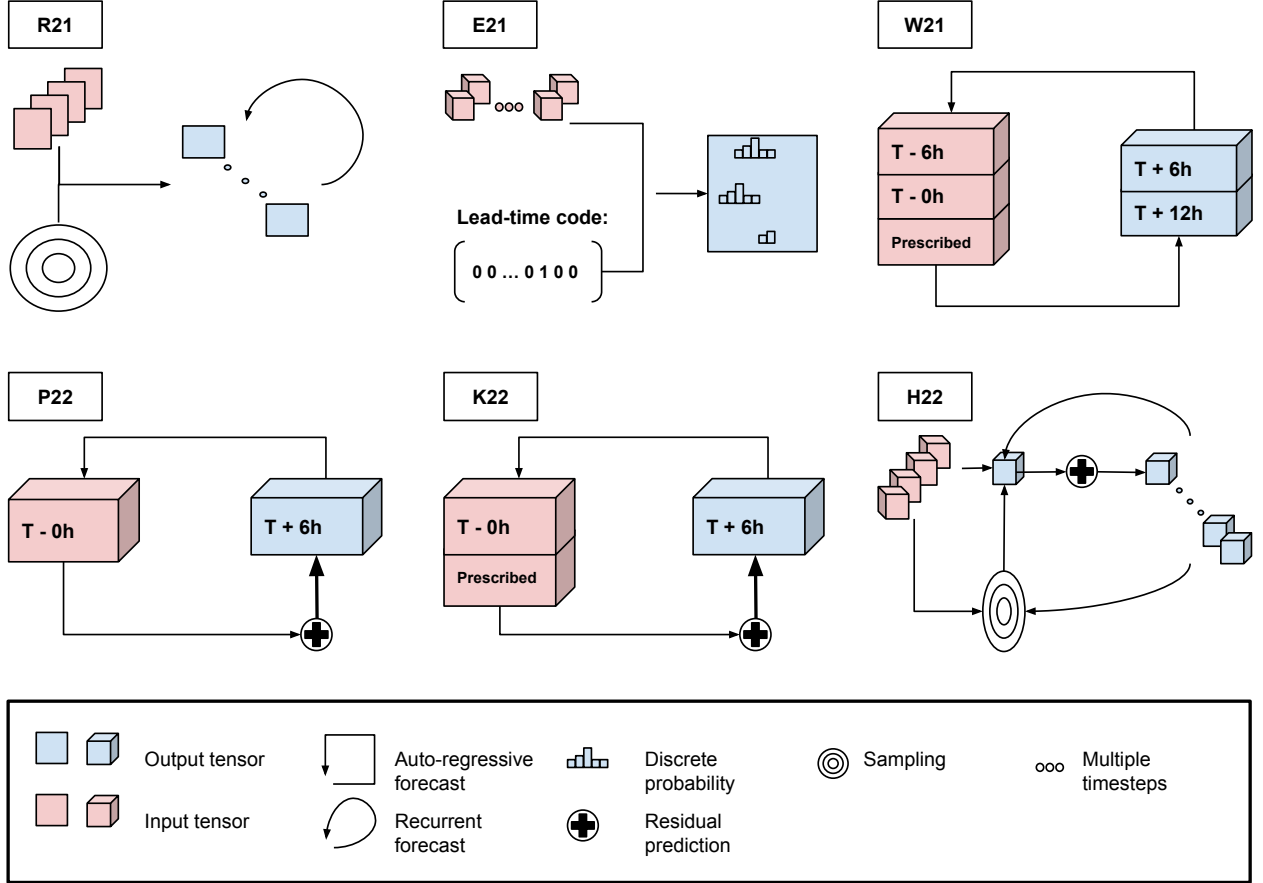


Figure 1: Objective definitions in the six reviewed models. Iterative forecasting models re-use their own predictions as input and are either (first-order) auto-regressive (W21, P22, K22) or incorporate a recurrent internal state (R21, H22). Residual predictions are added to the current input to produce the next state, maintaining all information that does not need to be changed. E21 directly predict at a lead-time specified by a one-hot code. Furthermore, they output probabilities over bins of the target variable. Generative models (R21, H22) involve a sampling step to model noisy perturbations of the forecast trajectories. They can thus be used directly to generate an ensemble of predictions.

In DLWP, both kinds of iterative approaches find application, depending on the desired forecast horizon. Short forecasts, e.g., in P22, W21, and K22, are generated auto-regressively, whereas H22 and R21 employ recurrent forecasts to operate over longer time spans (20 and 18 steps into the future, respectively), at the cost of a coarser spatial resolution. An interesting difference in the forecasting objectives arises from the use of residuals or absolute value prediction — H22, K22 and P21 each model the residual *change* from one frame to the next, which allows the model to maintain the current state information, potentially freeing up model capacity [59, 60]. The residual between two frames can also be interpreted as an estimate of the velocity of the dynamics, a factor that is made explicitly available to the model by the use of two in- and output frames in W21.

### 2.2.2 Direct forecasts

Direct forecast models generate a prediction only for a particular target lead-time, without any intermediate predictions. The lack of intermediate predictions eliminates amplifying or vanishing gradient problems and emphasises those temporal features that are most salient for the targeted time scale. However, usually only a single time step is generated at a fixed lead-time, which constrains the forecast ability of these models to the lead time that was trained.

To enable the generation of smooth forecasts with lead time models, multiple models may be trained to predict the weather at different lead-times [49]. Alternatively, direct forecasts at different lead-times, termed continuous forecasts in [12], are possible if the target lead-time is included as conditioning information—either in the form of an input field [49, 61] or as input to a separate conditioning network, as in E21. This approach may be computationally cheaper

compared to training multiple direct models for different lead-times, because it allows sharing features that are useful at all forecast time-scales. Moreover, when the chosen lead-time encoding can refer to temporal intervals of flexible length, as is the case in E21, it may help the model to discover the sequential nature of their forecasts. In most recent work [19], an ensemble of fixed lead-time models was combined to enable the creation of iterative forecast with reduced auto-regressive dependency, effectively combining the optimisation efficiency of direct forecasts with the generalizability of iterative models.

### 2.2.3 Probabilistic forecasts

Quantifying the uncertainty in a forecast plays an important role in all weather prediction tasks, especially for long forecast horizons. While NWP typically capture model uncertainty indirectly via random perturbations of initial conditions [62], DLWPs can directly capture model uncertainty either by producing probabilistic forecasts or by generating forecast ensembles via probabilistic generative models, as done in H22.

Probabilistic generative models [63] are DL methods that can be used to sample new data instances with statistics that (ideally) fit the distribution of the original data. Generative approaches obtain samples from a distribution that is easy to sample from (e.g., a standardised Gaussian) and apply a learned transformation on these samples to produce outputs with desired statistics [64]. The so-called reparametrisation trick [65] enables the effective training of such models from individual statistical samples of model predictions. Generative Adversarial Networks (GANs, [66]) and Variational Auto-Encoders (VAE [65]) are the currently most well-established generative DL approaches, while normalising flows [67, 68] and diffusion models [69] are currently emerging in DL as promising developments, but have not yet been applied to DLWP.

Both recurrent forecasting models, H22 and R21, also utilise a generative component, which was found to be crucial to account for the uncertainty inherent in long-term recurrent video prediction [70, 71]. R21 utilises a GAN to generate low-dimensional latent samples from a standard normal distribution, which then conditions all forecast steps equally on the largest represented scale. Similar mechanisms have been applied successfully for video generation [72]. Elsewhere, GANs have been successfully employed for the generation of both super-resolutions of atmospheric fields [73–75] and extreme event forecasts [76, 77].

H22, on the other hand, implements a dynamic VAE, where a stochastic perturbation of the latent memory state is sampled at each forecast step. [Girin et al.](#) review the family of dynamical VAE models in-depth. The statistics of the sampling distribution are learned by the neural network itself: based on the current input and the recurrent latent system state, a prior density is generated, which predicts the model's uncertainty. The prior density is adapted towards the experienced posterior density via a KL divergence loss (see below). The posterior density, on the other hand, is estimated directly given the successive input and the system's previous latent state. Similar mechanisms have been recently applied for latent model learning tackling model-based reinforcement learning tasks [79, 80].

As an alternative to modelling uncertainty internally, the output of a DL model can be formulated as, e.g., a mean and variance, or a probability over discrete bins, as is done in E21. In this case, the model's objective is to quantify its predictive uncertainty in combination with the forecast.

## 2.3 Loss function

Once the objective is defined, a loss function has to be chosen that will be minimised during training. Figure 2 illustrates the losses applied in the reviewed works. In practice, the quality of the model predictions is often verified with several metrics and additionally with case studies. Hence, it may be desirable to train the model with a loss function that reflects the most important, task-specific, properties for verification. To this end, loss functions that account for uncertainty and/or model a larger spatiotemporal extent may be considered.

### 2.3.1 Distribution of variables

When predicting atmospheric fields, the targets usually are continuous variables distributed over space and time. The standard approach to calculate the loss with respect to the objective is to discretise the target values in space and time via a spatiotemporal grid or mesh. Losses then typically target minimising a distance between the predicted and true data values, averaged over discretised space and time. Standard distance measures on real numbers are the L1- and L2-norm, that is, mean-absolute error (MAE) and mean-squared error (MSE), respectively. From a Bayesian optimisation perspective, the choice of norm relates to an assumption about the distribution of measurement noise or forecast uncertainty [81]. That is, under the assumption of Gaussian noise, the MSE is appropriate, whereas if we expect heavy tailed noise following a Laplace distribution, the MAE is adequate. Among the reviewed models, and in DLWPs in general, the MSE is the predominantly employed loss function. It finds application in W21, P22, K22,

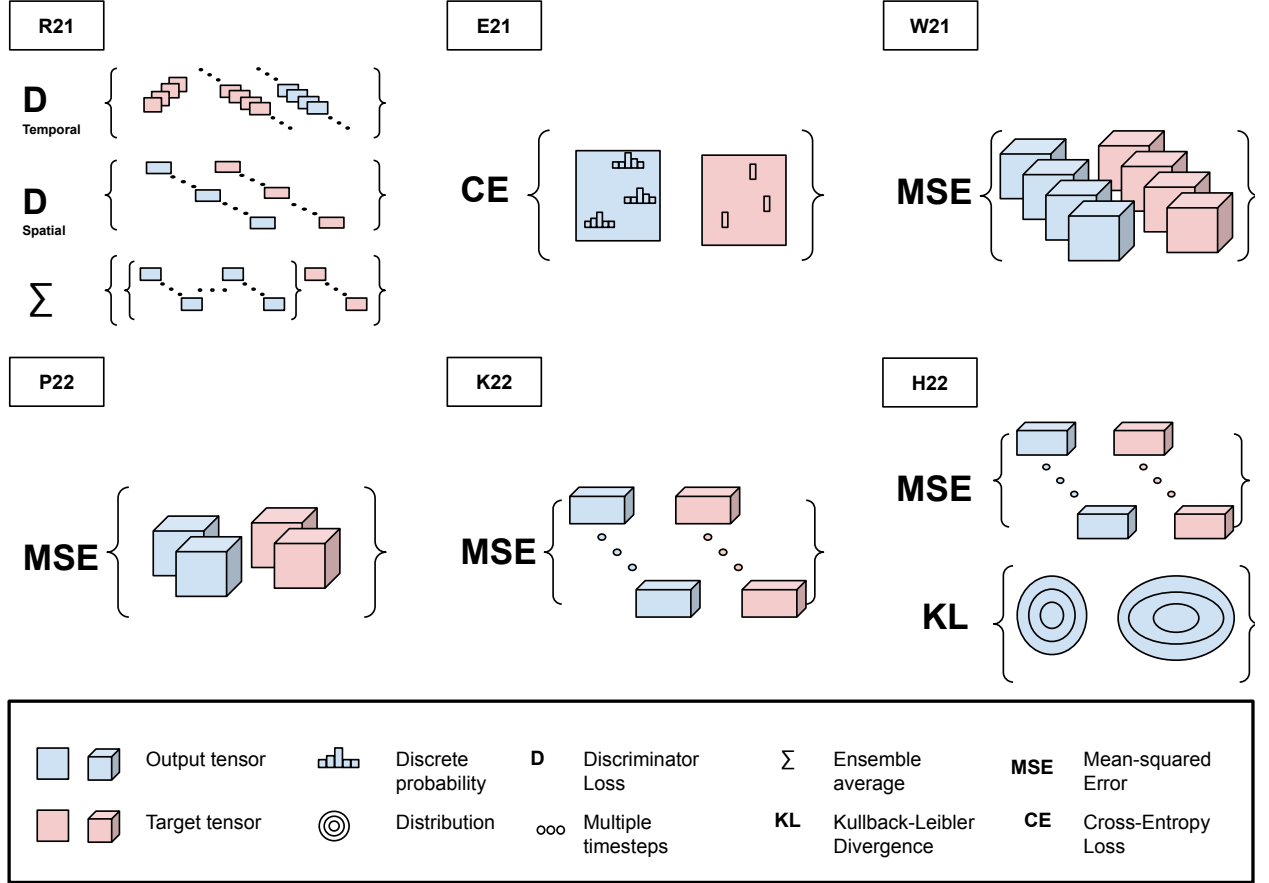


Figure 2: Loss functions used in the six models under consideration. Four of the six models rely on MSE, focusing on a small set of future states. R21, as a GAN, is trained via additional temporal and spatial discriminative loss components, besides an ensemble-average of errors. H22, as the other generative model, additionally includes a KL loss term, which leads to the optimisation of a prior uncertainty estimate. Finally, E21 uses the cross entropy loss, predicting distributions over precipitation intensities.

and H22, differing only in the forecast horizon, that is, the temporal extent of the loss computation. R21’s generative method differs in that it produces an ensemble of forecasts, where the mean of the ensemble is optimised to match the ground truth via the MSE.

Regardless of which pixel-wise metric is applied exactly, it is necessary to account for the fact that each variable will have its characteristic value range. In weather prediction, these ranges often depend on geographical location and pressure level. If these differences are not accounted for by appropriate normalisation, the loss will be dominated by the variables with the largest value ranges. K22, for example, re-scaled each variable to unit variance with respect to its 3-hour temporal difference, averaged over space and time. The most recent work in [20] follows a similar approach to support uniform model performance across variables. Further, the loss function of global forecasts is commonly re-scaled per spatial location to account for differences in area per pixel induced by the sphere to grid mapping in, e.g., ERA5.

When facing heavy-tailed variables, like precipitation or surface winds, standard MSE will penalise imprecise predictions of tail events quadratically, which tends to over-emphasise relatively small errors in the more extreme value ranges. Forecasts of precipitation thus benefit from the MAE or dedicated re-weighting schemes that emphasise accurate extreme event prediction [82, 83]. A log-transformation of heavy-tailed variables (or an according treatment in the loss function) has been shown beneficial [49, 84]. Alternatively, the target variable may be discretised, e.g., into quantiles, which turns the task into a classification, as demonstrated in E21 and its predecessor [61]. In this discretised case, the Cross-Entropy loss is applied effectively interpreting predictions as a probability density over discrete classes (i.e., quantiles). As a result, multi-modal densities can be generated to maximise the likelihood of the data given the model

output. Although not directly suitable for iterative forecasting, this approach can seamlessly account for heavy-tails and is agnostic to small variations that may be irrelevant or simply unpredictable.

### 2.3.2 Spatiotemporal extent

Aiming at minimising the average of any pixel-wise loss creates two main challenges. First, if the model predictions are even slightly offset spatially or temporally, this will produce a large error. Even worse, the large offset error will be counted at both, the predicted and the ground truth location, an effect that is known as the 'double penalty' problem [85]. As a result, when exact spatiotemporal forecasts are impossible, DL systems tend to regress to the mean [86], essentially blurring the prediction [87]. Second, especially in systems which show exponential divergence of nearby initial trajectories, the prediction of fine-scale features becomes impossible further into the future, causing the model to attempt to fit non-existing patterns and harming generalisation [57]. Ideally, with increasing lead-time, the model would focus on large-scale rather than on fine-grained feature accuracy. Since pixel-wise losses are agnostic to non-local, large-scale structures, they may encourage the model to attempt to fit unexplainable fine-scale data dynamics. Probabilistic and feature-wise loss functions can help tackle these challenges.

**Probabilistic loss functions** A loss function that explicitly represents uncertainty allows the model to predict fine-grained features and potential dynamics that are plausible, even if they differ from the observations. Probabilistic forecasts are also desirable from an operational point of view [30], but their calibration (i.e., how well the probabilities capture the true uncertainty) has to be investigated carefully [62, 88, 89].

Probabilistic loss functions are derived from the theory of maximum likelihood estimation. They either define the likelihood of a sample to come from a distribution or aim at minimising divergences between two distributions. Focusing on model likelihood given data, the negative-log-likelihood (NLL) or cross-entropy loss can be applied. NLL essentially evaluates the likelihood of the target stemming, for example, from a normal distribution  $\mathcal{N}(\mu, \sigma)$  predicted by a DL model [90, 91]. It should be noted that when facing input-dependent uncertainty variations, which naturally occur in weather dynamics, suitable normalisation techniques should be applied to NLL to avoid model collapse to highly uncertain predictions [92]. In contrast to the application of NLL with continuous densities, the cross-entropy loss can be used to optimise discretised densities. E21, for example, applies a cross-entropy loss over precipitation bins, enabling the prediction of multi-modal densities in their precipitation forecasts.

When aiming at minimising divergences between a latent and a desired distribution, an additional Kullback-Leibler (KL) divergence-based loss is typically used. In the case of a VAE, for example, the desired prior distribution is the standard normal distribution, encouraging latent standard normal-distributed generative encodings [65, 93]. Instead of inducing a fixed variational prior, as in VAEs, H22 learn to approximate the posterior model uncertainty via a prior density and employ a KL-loss to adapt its prior model uncertainty estimate to its posterior estimate, as detailed above.

A predictive distribution output by the model may alternatively be evaluated by proper scoring rules, such as the Continuous Ranked Probability Score (CRPS) or the Ranked Probability Score (RPS). Both of these metrics are commonly used to verify ensemble forecasts and probabilistic forecasts in meteorology [94, 95] and have also been used as loss functions for training DLWP models e.g. in [96, 97]. Among the reviewed models, CRPS and RPS are only used as a verification metric for both, probabilistic model outputs (E21) and ensemble forecasts (R21, W21, P22 and H22).

**Feature-wise loss functions** Feature-wise losses, sometimes called perceptual losses, aim at capturing extended structures in the data. Here, we differentiate between feature-wise losses that are calculated in the native data space and those that are calculated in the latent space of a DL model.

Spatial-verification (SV) metrics, which have a long history in computer vision [98, 99] and meteorology [85, 100, 101], are an example of a feature-wise loss in data space. They can be employed to identify best local pixel correspondences between images. As a result, such metrics encourage matching value distributions while allowing spatial imprecision.

Over the last years, they were successfully used to train DL models that produce high fidelity predictions in computer vision [102] and DLWP [103]. [104] offers a more in-depth discussion.

Latent feature losses are currently at the cutting edge of developments in DL and include GAN discriminators [66], contrastive losses [105, 106], or joint-embedding losses [107]. DLWP-related applications, such as super-resolution (statistical downscaling), have applied GAN-losses [73, 76, 77, 108] and in [109] a joint-embedding method was found to further improve super-resolution performance. In R21, two discriminator losses are optimised jointly to account for spatial and temporal aspects of the forecast [72], thus encouraging the generation of realistic-looking forecasts, which indeed were highly appreciated by expert weather forecasters.

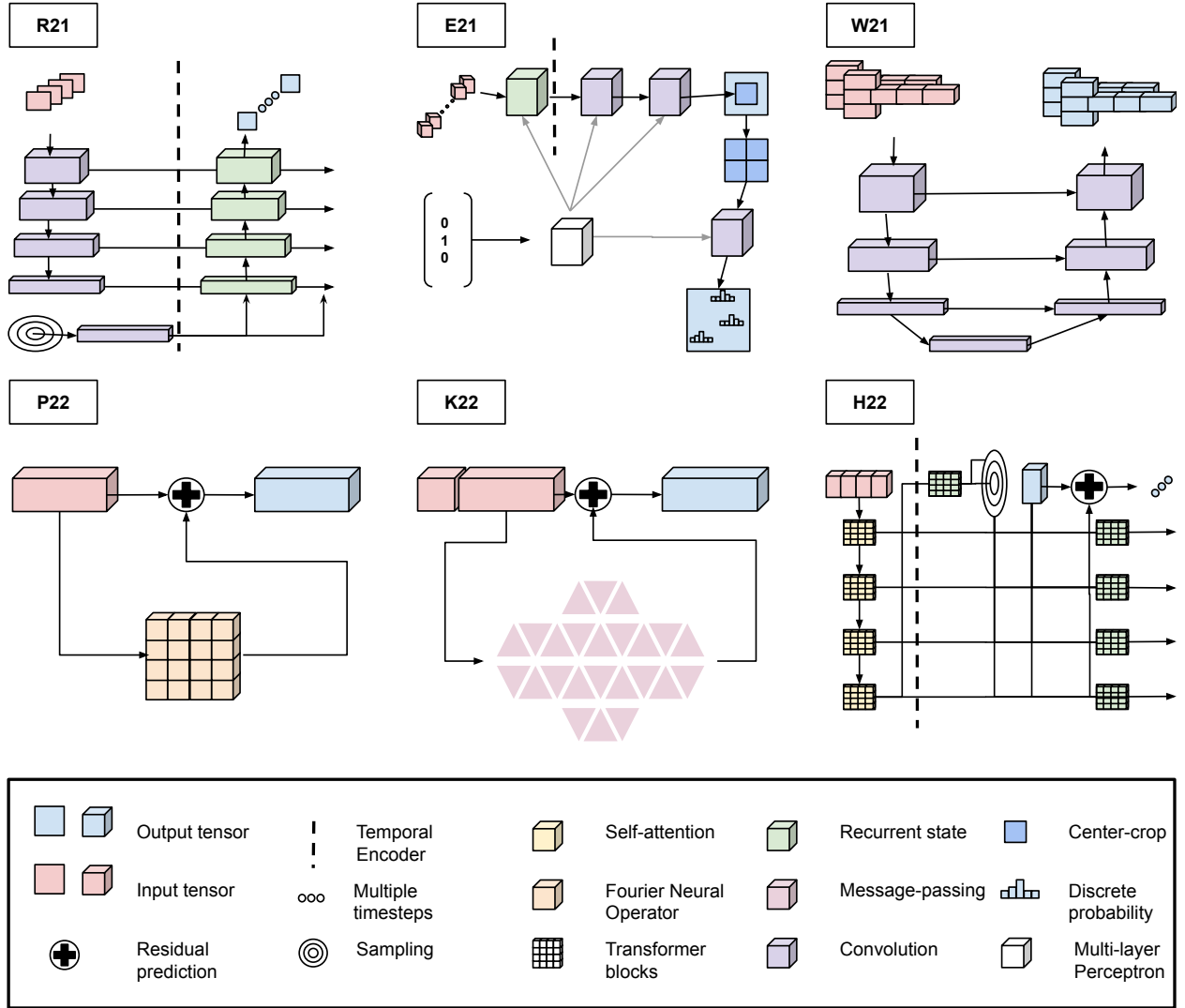


Figure 3: Architecture overview of the six reviewed models. Spatial multi-scale processing is explicitly encoded in R21, W21 and H22, whereas P22 and E21 rely on large (semi-global) receptive fields. Temporal processing is done via a Sequence-to-Sequence model in R21, E21 and H22, in contrast to the auto-regressive prediction models (W21, P22, K22). For detailed explanations and illustrations of the respective architectures we refer to the figures in their original papers.

## 2.4 Neural network architecture

In DLWP, the main components of the artificial neural network architecture typically consist of an encoder, a latent processing module, and a decoder. Each of these components in turn consists of finer processing modules and processing layers. The arrangement of these components and the specific processing modules impose a particular inductive bias reflecting assumptions about the data's structure and its spatiotemporal dynamics. A visualisation of the architectures of the reviewed models is presented in [Figure 3](#), for visual clarity we chose to omit block internal designs and layer depths and only highlighted dedicated spatial or temporal scales.

We now detail design choices with respect to encoding, dynamics processing, and decoding modules. Furthermore, we address the design of computational blocks which is an important aspect of best practices in engineering a neural network architecture.

### 2.4.1 Encoding

DLWPs typically first embed the spatiotemporal data into, potentially lower-dimensional, latent feature spaces. An embedding can be understood as a summary or an abstraction of the data values. The latent embeddings condense or interpolate information, restructuring and compressing the data for the chosen objective, which is quantified by the loss function. As a result, only the most prediction-relevant aspects of the current atmospheric state will be encoded and the self-organised latent representations may not correspond to particular data values or physical states. This encoder-decoder structure can drastically reduce subsequent computational processing load and concentrate processing power on the most task-relevant aspects, but makes verification of the model computations difficult.

**Data embeddings** DLWP model inputs are usually organised as tensors with spatial, temporal, and channel dimensions. Gridded tensor representations implicitly assume a uniform distribution of locations on a rectangular grid. Global earth observation data, for example the widely used ERA5 [Section 2.1.2](#)), this assumption causes the area of polar regions to be over represented and causes a boundary artefact on the dateline. A fundamental design choice lies in how to deal with these distortions in DLWP architectures.

During pre-processing W21 map the rectangular data onto the six faces of a cube surrounding the sphere. This cubed sphere format reduces distortions and irregularities from the data and incorporates appropriate cyclical boundaries. K22 defines an icosahedral mesh [\[110\]](#) which approximates the earth's spherical shape with few distortions. Mapping to and from the rectangular data grid to the spherical mesh-grid is done with a learned encoder and decoder component and the main processing of the network occurs on this latent mesh-grid.

The other four models do not provide direct architectural adaptations to the shape of the earth. R21 and E21 focus on local regions and are thus less affected by these distortions. H22 and P22 rely on a learned patch-embedding scheme where the grid locations are first aggregated into non-overlapping patches, as initially proposed in [\[111\]](#). The pixel-wise values are linearly mapped onto the channel dimension, similar to the space-to-depth and depth-to-space operations employed by R21. Note, that this initial embedding is explicitly not a compression. Patch embeddings do not directly account for distortions, but they are commonly combined with location-specific information during processing (c.f. [Section 2.4.2](#)), which may alleviate these issues to some extent.

**Latent embeddings** Besides the handling of distortions via the DLWP architecture, the encoding design choices foster the emergence of particular spatiotemporal representations. Seeing that natural processes, such as weather systems, can be well-described on multiple spatiotemporal scales, a strong inductive bias for multi-scale processing comes with an internal encoding that consists of a hierarchy of embedding layers.

A prime example of such a multi-scale processing architecture is the U-Net [\[112\]](#), which was originally designed for medical image segmentation. U-nets include skip-connections between different stages of the encoder and the corresponding stages of the decoder, which is essential to maintain the information at each intermediate scale. More recently, additional skip-connections have been introduced to model dependencies between several scales and intermediate resolutions [\[113–115\]](#). U-Nets are currently the most widely employed architecture in DLWP [\[116\]](#). The low-dimensional embeddings of U-Nets make them particularly efficient convolutional neural networks (CNN) for dense prediction tasks. Moreover, their multi-scale structure exhibits a natural inductive bias for the hierarchical processing of atmospheric dynamics, e.g. [\[21, 82, 84, 117–120\]](#). The work of W21 [\[7, 23, 121\]](#) is fully U-Net based and both R21 and H22 utilise this structure, too, although H22 note that the benefit of multiple spatial scales in their model was marginal.

DL architectures that are designed to map between time series as both input and output are called Sequence-to-sequence models. In their original form [\[122, 123\]](#) they compress the entire input sequence into a representation of a single state which then forms the initial state of a sequence generating decoder. Temporally long-range interactions may

be achieved by a latent memory state as in gated RNN [55, 124, 125] or through attention over past states as in the Transformer [126], which itself is a form of RNN [127]). Sequence-to-sequence models are strictly more expressive than time series prediction models without an encoder-decoder approach [128] and can e.g. operate on different input and output time scales.

Both recurrent forecasting models (R21, H22) operate as Sequence-to-sequence models in addition to their spatial multi-scale structure. In R21 each input frame is first processed in parallel and hierarchically by the convolutional encoder and the individual frame representations are then concatenated and further processed to yield the initial state of the recurrent decoder. E21 receives an even larger set of information about the recent past, which is aggregated via a convolutional LSTM-based recurrent neural network [5] without imposing explicit hierarchical structures. H22 fuse the temporal information of multiple past states during the initial patch embedding and hierarchically generate multiple spatial scales afterwards to form the initial state of the recurrent predictor.

Neither P22 nor K22 incorporate specific structures in their internal embeddings. Instead, these models rely on the emergence of suitable spatiotemporal patterns purely through their learned dynamics processing modules.

#### 2.4.2 Dynamics processing

Depending on the encoding, the latent state encodes particular receptive fields, which refers to the neighbourhood from which information may be integrated. In DLWP, and spatiotemporal modelling in general, we have to choose the receptive field carefully to be able to model the relevant dynamical patterns. The encoding of excessively large receptive fields quickly becomes prohibitively expensive in terms of computational resources needed and loses the important inductive bias towards local processing. Choosing the receptive field too small will restrict the model and prevent relevant, large-scale patterns from being captured.

The trade-off between receptive field size, local inductive bias and computational efficiency, poses a substantial challenge for atmospheric dynamics where all scales may contain predictive information [129, 130]. Regardless of a grid or graph structure, the encoded receptive field will inevitably depend on the chosen temporal resolution and spatial discretisation of the data (cf. CFL condition [131] in NWP).

**Grids** Convolution-based models [132], such as R21, E21, and W21, construct their receptive fields from small ( $3 \times 3$ ) sliding windows (kernels) over a regularly spaced grid. Larger receptive fields emerge only as a consequence of hierarchical latent space encodings and depth, that is, the number of successive convolutional layers. E21, who do not impose a hierarchical encoding, capture large-scale structures via convolutions with an increasing dilation factor [133], which spreads the pixels in the sliding window to exponentially wider areas without increasing the number of integrated pixels.

An alternative to convolution-based models are Transformers [126], which have been originally proposed for sequence modelling, but were further adapted to computer vision yielding state-of-the-art performance [111]. In DLWP, Transformers have just begun to emerge in, e.g., the works of H22 and Bi et al.. Transformers apply an attention mechanism that evaluates similarities between locations in the form of queries and keys and then propagates values weighted by the determined similarities. Such a mechanism has a quadratic complexity in the number of locations that are being compared and quickly becomes impracticable when attempting e.g. to compare all pixels in a high resolution grid. One adaptation that helped to alleviate this problem is implementing attention only within shifted-windows [134]. By utilising slightly overlapping windows, global interactions with few intermediate processing steps become possible. For further approaches to reduce the computational complexity of global Transformers, as used, e.g., in [61] for precipitation forecasting, we recommend the review by Tay et al..

The Fourier Neural Operator [136] and its adaptive variation [137] that is used by P22, enables a grid-based convolution with a global receptive field at quasi-linear computational complexity. To achieve this reduced complexity, the Discrete Fourier Transformation is used to map the grid to the domain of spatial frequencies and back again. In the Fourier space, P22 applies an MLP to integrate information across all frequencies and thus across space. This corresponds to a convolution with a global receptive field. Since the frequencies are not crucially dependent on the discretisation of the grid (at least up to a certain scale), these models can be trained and evaluated on different grid resolutions, which is not possible with standard convolutions.

**Graphs** In contrast to grids, graphs offer a more flexible structure for defining neighbourhoods on geometric objects [138]. In graphs, spatiotemporal locations are the nodes of the graph and edges between these locations represent potential, pair-wise, interactions [22]. In graph neural networks (GNN), these interactions are modelled by the message-passing framework [139], which first computes a ‘message’ that travels along each edge, and then integrates all incoming messages at a node. Both computations are usually learned by MLPs, although linear GNN have recently been shown

to be promising in other applications [140–142]. Interestingly, the graph message-passing framework can be seen as a learned form of the Finite Element Method [143].

K22 utilises message-passing on a mesh-grid, which has previously been used successfully in simulations of fluid dynamics [144–146]. More recently, the same framework was extended by [20] to achieve state-of-the-art performance in medium-range weather prediction. In the future, the flexibility of the message-passing framework could potentially enable connectivity patterns that account for mountain ranges, coast lines, and other domain-specific factors (see e.g. [147] for a climate application of graph structures).

Note that a uniform grid is a special case of a graph and thus it is possible to express the function learned by a grid-based model, like a CNN, as a graph-based model, like a Transformer, but not vice versa [148]. In fact, Transformer-based models such as H22 may be seen as a special case of a fully-connected graph structure [149] where the input tokens are equivalent to nodes, edges exist between all nodes [150], and the weights of the edges are dynamically computed from the data [151, 152].

All of the approaches discussed so far restrict themselves to defining graphs over the spatial domain only. In previous work on video understanding in Transformers [153] and spatiotemporal graphs [154] it has been shown that including both spatial and temporal aspects into the model can lead to substantial improvements. Similar approaches may help to further emphasise temporal, besides spatial and hierarchical, structures in DLWPs.

**Positional embeddings** Although the physical laws that govern our weather are location invariant, boundary conditions play an important role. For example, atmospheric dynamics evolve differently over land and ocean. Information about the global position in a grid or mesh may thus be useful to compute interactions and generate predictions. Additionally, local information, such as land cover and orography, may be used to condition the spatiotemporal processing dynamics further [155, 156].

Convolutional models directly account for the relative position through their fixed-size sliding window, inducing a locality-oriented inductive bias that learns translation-invariant features. Absolute position usually has to be provided as an input, e.g., in the form of geospatial coordinates—even if convolutional models may infer the distance to a zero-padded boundary [157], thus indirectly inferring their absolute positions.

Graph-based models [158] and Transformers [126] are permutation invariant and thus do not consider relative or absolute positions in their computation. For DLWPs, and many other applications, this is an undesirable property. Thus, additional features are provided that encode either the absolute or relative position of graph nodes or tokens

K22 incorporates not only geospatial coordinates and orography as input, but also encodes the relative distances and sizes of nodes and edges in the graph. H22 encodes relative distances as learnable parameters and P22 use an absolute position encoding, both are common methods in Transformer models. Most recently, an earth-specific location embedding was implemented successfully [19], highlighting the potential for future developments in this direction.

### 2.4.3 Decoding

The decoding stage of DLWPs projects their dynamic latent state predictions back into data space. Often, up-sampling is applied to predict the data on a finer scale than that used in dynamic processing.

R21 up-samples its hierarchical, latent state predictions during processing. A final block of several convolutions and one depth-to-space layer linearly maps channels to locations and yields the individual radar signal forecasts. E21 focuses on predicting precipitation within the inner target area of  $512 \times 512$ km, starting with an input field of  $2048 \times 2048$ km. To do so, the latent prediction of size  $512 \times 512$  is first centre-cropped ( $128 \times 128$ ) and then up-sampled to  $512 \times 512$ km and the final categorical probabilities over binned rain intensities are computed as output. W21’s decoding routine is contained in the U-Net up-sampling path, directly yielding successive state estimates. P22 uses a linear decoder, which splits the initial patch embedding into individual grid locations and projects the predicted dynamics back onto the data space. K22 decode the icosahedral graph network output back into gridded physical variable changes via a final GNN decoder that aggregates information from the three closest mesh-nodes. H22 employs a Swin block to decode the output from all of its hierarchically-arranged recurrent prediction modules and then splits the initial patch embedding back into individual grid locations.

In DLWP the last layer of the network is almost always a linear regression from the latent space channels to the data-channels. An implicit inductive bias of all of these models is that the prediction is a linear combination of the representation of the final layer. Decoding may thus be viewed as the least sophisticated architectural component. However, it should be remembered that the chosen data representation (Section 2.1) and loss function (Section 2.3) both induce important additional inductive biases on the model output.

#### 2.4.4 Computational blocks

Besides the distinction between grid and graph structures and the processed spatiotemporal dynamics within, further considerations can yield additional beneficial architectural design choices.

Common practice in the development of deep neural networks is to organise multiple layers into computational blocks that are repeated throughout the network. Block design eases the implementation and engineering process and facilitates transfer of well-working components between different architectures. For example the Swin-block used in H22 is based on the original Transformer block of [126] which was further adapted by [134]. Similarly, the computational blocks used by R21, E22, and K22, and P22 follow, or slightly modify, existing designs. We now discuss two important components of all block designs implemented by the reviewed models, namely residual connections and normalisation layers.

A core advancement in the history of DL was the introduction of residual blocks, that combine the input and output of a computational block in an additive manner [159]. Residual connections preserve high resolution information, facilitate the propagation of gradient information to early encoding layers, and thus avoid the vanishing gradient problem and enabled the training of very deep neural networks [160]. As a result, residual blocks are now used in essentially all modern DL architectures.

Besides data normalisation, discussed in [Section 2.3](#), dedicated normalisation modules between (or after) the projection and the non-linearity within a processing block may be applied [161–166]. Empirically, it has been found that normalisation leads to faster and more stable convergence (for a theoretical perspective see e.g. [167]). Normalisation re-scales all intermediate activations within a layer to have zero mean and unit variance. Various forms of normalisation differ along which dimensions they calculate the reference statistics (see [163] for a comparison). Among the reviewed models, P22, K22, and E21, and H22 utilise normalisation over the channel and spatial dimensions, whereas R21 use normalisation over the batch dimension and W21 omit internal normalisation entirely.

Immediately after the normalisation, an affine transformation with learned parameters is often applied to allow the activation statistics to be adapted to the data. Recent work in [166] and [168, 169] suggests that learned affine parameters may achieve the beneficial effects of normalisation by themselves. In E21, for example, the parameters of the affine transformation are predicted by a secondary neural network based on the targeted forecast lead-time, which enables maximally effective, layer-specific lead-time encodings. The same principle has been used in previous work [170, 171] to condition on various kinds of auxiliary information, an approach that could hold promise in DLWP for integrating other relevant data sources.

### 2.5 Optimisation

Once a suitable learning problem has been formalised, the parameters of the DL model are optimised such that they best represent the objective function. Neural networks are trained via gradient descent on the loss surface, which is defined by the loss function, the data and the network architecture. Interestingly, the choice of the optimisation method is an inductive bias itself [172]. We briefly discuss intuitions about the loss surface, the benefits of overparameterisation, and the importance of learning rates, which are common to all DL models. Next, we discuss various curriculum learning strategies, defined as sequences of intermediate objectives that facilitate the learning of, e.g., complex spatiotemporal dynamics. Finally, ensembles depict a critical component of modern NWP and we will discuss various ensemble methods in the context of DLWP.

#### 2.5.1 Stochastic gradient descent

Stochastic gradient descent (SGD [173, 174]) is the backbone of all DL optimisation schemes. By sampling small subsets of data (batches) and updating model parameters corresponding to the steepest descent on the loss surface with respect to each batch, SGD traverses the loss surface [175] in a stochastic manner. The stochasticity allows escaping from local minima, which otherwise often pose a substantial issue for gradient-based optimisation. Intuitively, the minimisation of the training loss for one batch may be sub-optimal for another, such that the SGD will only remain in regions of the loss surface that are suitable for a wide range of batches, which are more likely to generalise well [176, 177].

**Overparameterisation** DL models today use up to billions of parameters, a fact often met with suspicion by researchers with a background in classical statistical theory [178]. Recent findings (as reviewed in [172]) suggest that overparameterisation itself may be an inductive bias that facilitates convergence of SGD towards well-behaved solutions. Indeed, it has been shown, both empirically [179] and theoretically [180, 181], that vastly overparameterised models can often generalise better to unseen data than smaller models and are more efficient learners in terms of data

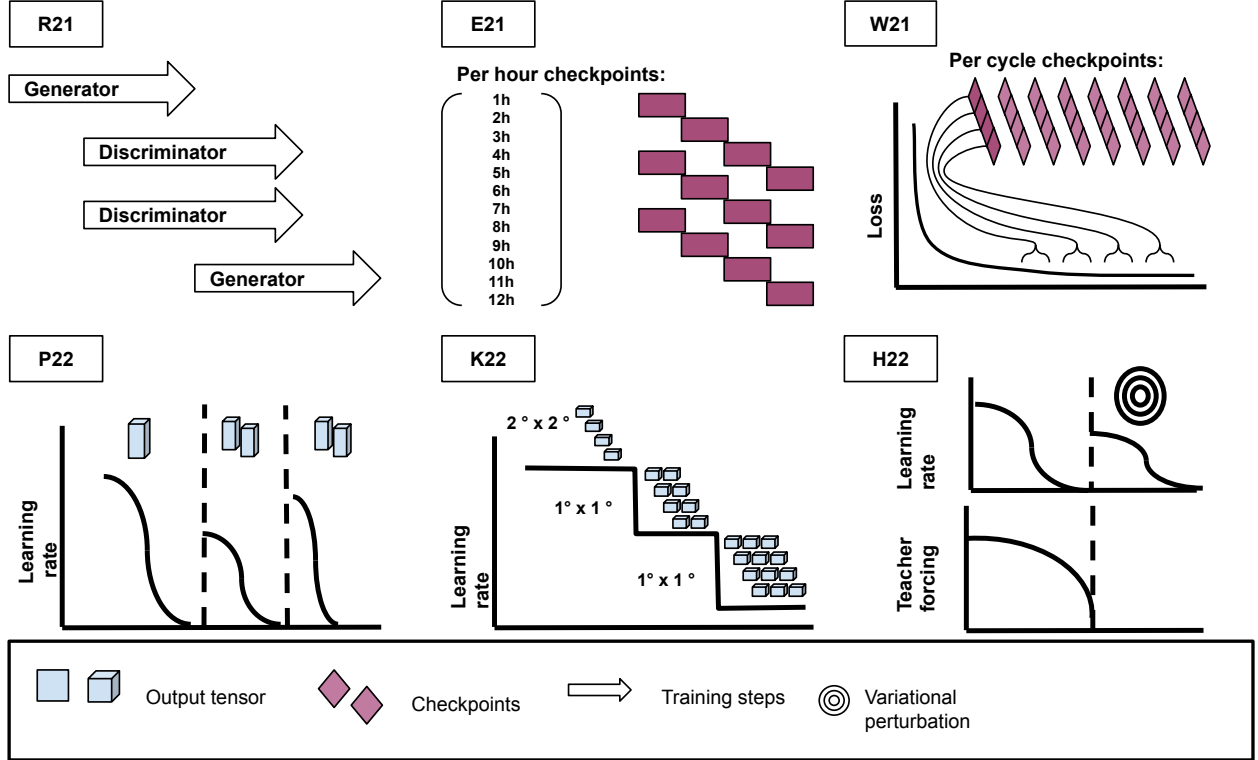


Figure 4: Training schemes of the six considered models. R21 alternate between discriminator and generator optimisation. E21 and W21 create checkpoints, to keep track of best models and (in W21) to construct an ensemble. P22 employ a curriculum learning approach starting with pre-training on predicting  $t + 6$ , to later predict both  $t + 6$  and  $t + 12$ . Moreover, P22 apply a cosine scheduled learning rate and lower the learning rate when predicting  $t + 6$  and  $t + 12$ . For further fine tuning, P22 adds a precipitation model, which we do not cover in further detail here. K22 report benefits from a coarse-to-fine optimisation curriculum and also a lowering of the applied learning rate. Finally, H22 apply a curriculum learning approach, activating the perturbation model only later during training and relying progressively less on so-called teacher forcing, that is, feeding in true data instead of own predictions over time.

and compute resources [182]. Following up on [182], however, [183] re-emphasised the importance of the amount of training data while confirming the sample efficiency of overparameterised models.

Current state-of-the-art DLWP models, too, are heavily parameterised: The smallest model, W21, has 2.7 million parameters. Given what is currently known about the scaling behaviour of DL models [184], it is likely that future work will improve the generalisation behaviour far beyond its current state when training much larger models on even larger shares of the vast amount of available data (e.g., in ERA5 and CMIP6).

**Learning rates** The learning rate, which determines the size of each parameter’s update step, is the fundamental hyper-parameter that has to be chosen for optimal convergence of SGD. Note that the actual step size is equally dependent on the batch-size, where larger batch sizes generally correspond to smaller effective learning rates [185, 186]. Adaptive step sizes are widely used to speed up the training process, for example in the very popular Adam [187] and AdamW [188] optimisers, which combine SGD with parameter-dependent momentum [189] and adaptive step sizes. Due to large movements of SGD (and related algorithms) which allow to jump over minima, the learning rate has to be decreased for the optimisation procedure to fully converge. Various schemes have been proposed to reduce (anneal) the learning rate, either as step-functions at pre-defined intervals or when a validation criterion is met, or as smoothly decreasing schedules, such as linear or cosine-based annealing [190]. Finally, increasing the learning rate, either initially [185, 191] or during training [190, 192] can improve generalisation performance and speed up optimisation substantially.

Among the reviewed DLWP models (c.f. figure 4), H22 and P22 utilise a cosine learning rate schedule, which is restarted following their curriculum learning strategy discussed below, whereas K22 uses a step schedule in combination with a curriculum learning strategy. The other models do not use learning rate annealing, but end the training after a fixed number of steps. Due to the differences in model convergence per target lead-time hour, E21 utilise per-hour checkpoints based on validation performance to ensure uniform performance across lead-times.

### 2.5.2 Curriculum learning

Curriculum learning [193] describes the idea that a sequence of increasingly challenging objectives may lead to better final models than immediately training on the main objective. Originally inspired by the way human learning works, pre-training is now a fundamental element of high performance DL [194, 195]. Essentially, curriculum learning may be seen as a sophisticated initialisation of model weights, beginning optimisation from a well-performing, instead of random, model configuration [196, 197].

Training at high spatiotemporal resolutions is computationally expensive and especially long temporal predictions often suffer from initial errors quickly amplifying and hindering training. Instead, curriculum training suggests to optimise only 1-step ahead predictions initially and include more expensive and complex temporal dynamics later. This approach is taken by P22, with an additional fine-tuning step for a precipitation forecasting module that operates on top of the auto-regressive atmospheric state predictions—since precipitation is a fast varying, highly stochastic variable, its inclusion in the atmospheric state prediction was considered harmful (also in [49]). H22 use a similar approach where the length of the forecast sequence is stochastic and longer sequences become increasingly likely during training—a procedure known as scheduled sampling [51, 52]. In addition, H22 only add their stochastic perturbation module once the model is generating sufficiently accurate deterministic forecasts. K22 uses an increasing number of auto-regressive steps during curriculum learning, but also performs a first round of training on coarse resolution data. The coarse initial training requires less resources and primes the model to consider large-scale spatial features, which may induce a useful bias towards considering multiple spatial scales, although the model does not explicitly contain different scales. The alternating optimisation of Generator and Discriminator (e.g., loss function) in R21 may be seen as an extreme case of curriculum learning, where the objective defined by the Discriminator becomes more challenging every time the generator was optimised and vice versa.

### 2.5.3 Multi-model ensembles

A common observation in machine learning, as well as in NWP and DLWP, is that an ensemble of predictors will outperform a single predictor [62, 81, 89]. Several methods have been developed in DL to enable efficient generation of ensemble forecasts, for example, by creating multiple deterministic models from different weight initialisations. Multiple training runs of neural networks generally produce different outcomes, owing to the randomness in the initial weight configuration and the batch-sampling in SGD. However, neural networks are expensive to train and obtaining a desirable number of ensemble members is often not feasible with a fixed computational budget. Stochastic model components, such as dropout [198] and related methods [199–201], can be used to implicitly train an ensemble of slightly different models jointly, but as noted in [89] and H22, the resulting ensembles are often sub-optimal. Conveniently, stochastic trajectories of SGD support a more efficient form of ensemble generation: Over several epochs, the model will likely jump between different, roughly equivalent, minima [202, 203]. Snapshots (or checkpoints) of the model at different times may be used to efficiently generate an ensemble [170]. Indeed, this is the approach taken by W21 to support efficient generation of a multi-model ensemble (32 models) from few training runs (8 runs). As discussed in [204], the use of cyclical learning rate schedules could improve this procedure further. In addition to their generative model, H22 train several model configurations to further improve ensemble statistics.

## 3 Discussion

At the time of writing, the most recently published DLWP models report forecasting skills that exceed state-of-the-art NWP models when evaluated on ERA5 data [19, 20]. Only a few years ago, it was not clear whether DLWP models would be capable of such high performance forecasts, especially on the challenging three to ten day forecasting range [205]. This rapid skill development is likely to continue in the near future as more resources are being invested and acknowledging that a fundamental strength of DL models lies in their ability to scale efficiently with compute and training data [181, 182]. Beyond computational scaling, though, further targeted research developments including DL designs will most likely yield further improvements. Besides combinations and optimisations of the techniques surveyed above, we expect that particularly the incorporation of physical domain knowledge and the quantification of uncertainty will be crucial. Together, these directions will improve the trustworthiness and interpretability of DLWP forecasts, which remain major challenges for an end-to-end DL weather forecasting system [206].

### 3.1 How physics can inform deep learning

Knowledge about the physical processes that underlie the weather and climate system is a crucial ingredient in DLWP models. Translating this knowledge into suitable inductive biases will in all likelihood further improve generalizability and enable more efficient training [207, 208]. Throughout [Section 2](#), we have seen how current DLWP model design is inspired by physics—primarily in the design of the scales of input, target, and latent representation, the choice of forecasting objective, and the spatiotemporal structure of both the loss and the network architecture. Such structural information is essential for efficient DLWP models, but it is not the only way in which physics could be incorporated.

A rich literature on physics-informed DL [209–211] outlines several other avenues. Explicit analytical constraints may inform the DLWP model about conservation laws like the conservation of energy and momentum. This approach has been explored thoroughly in the work of [212–214] and improved the generalisation of the models and the stability of neural sub-grid parameterisations. Additionally, a large variety of physics-informed neural networks (PINNs) have been developed in recent years, which, for example, can learn to solve partial differential equations analytically (PDEs) [215–217]. Less constrained approaches have been shown to successfully parameterise spatiotemporal PDEs that are encoding advection-diffusion-sorption processes, exhibiting strong generalisation performance as well as robust boundary condition inference [218, 219]. A recent review by [Cuomo et al.](#) provides further information about the current developments along these lines.

Approaches that explicitly incorporate physics, such as the ones mentioned above, have not been incorporated into large-scale DLWP models so far. The inherently high-dimensional, self-organised nature of neural latent spaces makes it difficult to assess the effectiveness of explicit physical constraints. Indeed, relying fully on the self-organisation capabilities of DL has been the way forward in most other domains where DL is highly successful, such as image and natural language processing. A promising direction, as pointed out in P22, is the development of Neural Operator models that are proving highly effective at solving partial-differential equations [136, 221].

In the context of DLWP, however, the concern remains that the governing equations ([Box 1](#)) are prohibitively challenging to solve exactly for the entire atmospheric system. Any approximation of these processes, however, will inevitably incur modelling errors [222]. For NWP, this realisation leads to the development of stochastic parameterisations [223, 224] and more recently reduced-precision models (e.g. [225–227]), which enable probabilistic forecasts that are less exact on the physical level but produce better forecasts. A similar stance might be taken by DLWP models, whose outputs may not exactly conform to the laws of physics, but which might be able to generate efficient, probabilistic forecasts that could ultimately prove more useful in operational practice [228].

### 3.2 How deep learning quantifies uncertainty

Predicting the future is inherently associated with uncertainty, especially in a high dimensional, complex system like the earth’s atmosphere. Forecasts that account for this uncertainty are ultimately more useful than purely deterministic forecasts, because they enable well-informed decisions to be made, even if the forecast turns out to be wrong [229]. Two major sources of uncertainty are present in weather prediction: (i) uncertainty about the initial conditions and (ii) uncertainty about unresolved processes [230].

Initial condition uncertainty results from incomplete and imprecise measurements, since it is impossible to fully observe the state of the atmosphere at all scales that may affect the dynamics. To account for this uncertainty, the initial conditions used in the model may be stochastically perturbed to generate an ensemble forecast and a straightforward way to generate perturbed initial conditions is through additive noise on small scales. For NWPs, though, such small-scale perturbations have been observed to be damped by the model dynamics, leading to underdispersive ensembles, which are typically overconfident in their forecast [62]. H22, W21 as well as [89] report similar observations. Perturbations along the directions of the singular vectors of a linearised adjoint model [231, 232] may result in a better ensemble spread. Generative models, such as R21 and H22, may be used to sample ensembles where the initial conditions are perturbed in a learned way and thus may capture non-linear and scale-specific tendencies.

Unresolved processes in NWP are addressed by parameterisations that can be further perturbed to obtain an ensemble. It is non-trivial, though, to generate perturbations that accurately reflect the correlations and the potentially complex interplay between different parameters. In DLWPs, unresolved processes are not modelled explicitly but instead their effects may be inferred by the model during the training procedure within its self-organising latent representations. In this way, the model parameters can potentially capture interactive effects and correlations between several unresolved processes.

### 3.3 Further into the future

The rapidly improving success over the past five years of DLWP in precipitation nowcasting and global weather forecasts are undoubtedly impressive. Yet, there is a wide range of temporal scales that are highly relevant from a societal perspective, but remain a challenge for the next generation of models. In the following, we argue for the necessity to extend the forecast horizon and to address the impacts of anthropogenic climate change.

**Extending the forecast horizon** A common issue with all the discussed models (except for W21) is their limited forecast horizon, not by the predictability of the atmosphere, but by the increasing ‘blurriness’ of predictions that ultimately leads to unrealistic and unusable model outputs. In [Section 2.3.2](#), we discussed how this effect arises from the well-known regression to the mean problem. The covered DLWPs have addressed this issue either through explicit probabilistic models (as in H22 and E21), or through feature-wise loss functions (e.g., R21 or [\[109\]](#)). However, a more fundamental issue is that the most common objective functions and training schemes emphasise the representation of spatial features, but neglect the rich temporal multi-scale structure of atmospheric dynamics. Explicitly accounting for dynamics that evolve over longer periods of time poses an engineering challenge, as it drastically increases the computational load, but also a representational challenge, as slower modes of atmospheric variability need to be captured by suitable representations of temporal dynamics.

Sub-seasonal to seasonal (S2S) scale forecasts are considered an important area for future developments of weather prediction in general [\[233, 234\]](#). An active interest lies in pursuing more data-driven methods [\[235, 236\]](#) and DLWP has been applied to S2S forecasts with some success (e.g. [\[21, 237\]](#)). Identifying and exploiting large-scale atmospheric patterns such as the Madden Julian Oscillation [\[238\]](#) and their global impacts [\[239\]](#) is a major source of S2S forecast skill [\[240\]](#) and a task that DLWP may be well suited for (e.g., [\[147, 241\]](#)).

On even longer time horizons, we enter the realm of future climate projections, where the primary task is to be able to model the response of the coupled ocean-atmosphere-biogeosphere system to climate forcings [\[242\]](#)). Predictions on climatic time scales are critical to support policy-making that addresses and anticipates the results of anthropogenic greenhouse gas forcing on the Earth system [\[243\]](#). DL in climate modelling often comes in the form of parameterisations for physical models (e.g. [\[15, 244\]](#)) but it is possible that future work could lead to end-to-end DL-based climate models [\[245\]](#). A further question for DLWP that arises from the changing climate is a matter of generalisation—can we expect that DLWP models will continue to work well if the distribution of weather statistics shifts dramatically? This question could be addressed either through explicit training on climate model data [\[246\]](#) or by incorporating the response to changing boundary conditions and climate forcings mechanisms such as greenhouse gas emissions into DLWP models (e.g. [\[247\]](#)).

**Foundation models** A promising ongoing research effort in the broader DL community is concerned with ‘Foundation Models’ [\[248\]](#). Extremely large models that are pre-trained have been found to exhibit impressive few-shot generalisation to various downstream applications. Indeed, recent results [\[249\]](#) highlight the potential of foundation models in the context of DLWP, especially as a tool for predicting longer time-scale phenomena and extreme events, for which less data is available. Key to the development of foundation models is the utilisation of self-supervised objectives, which have been shown to develop useful latent feature encodings for a variety of tasks [\[195, 250–253\]](#). The availability of large foundation models in DLWP could be a cornerstone for a wide range of crucial developments e.g., in the prediction of extreme events .

### 3.4 Concluding remarks

Deep learning for weather prediction (DLWP) is quickly establishing itself as a valuable paradigm for short-to-mid-range weather forecasting. State-of-the-art models are just beginning to outperform traditional methods and will likely continue to do so as they are scaled up and further refined. Here, we reviewed six impactful approaches that showcase the wide range of applicable methodology from the broader DL community and how these methods integrate weather-specific knowledge into their design. We believe that the presented template for discussing inductive biases and physics-informed design choices will be widely applicable beyond the models reviewed here. Although promising, the current crop of models are likely to be superseded by more accurate, efficient, and probabilistic forecasting models in the near future. Especially in the face of anthropogenic climate change and the resulting increase in the likelihood and intensity of extreme weather events, it is critical that weather forecasting models are as skilful as they can be to decrease the consequent humanitarian, biological, and economic losses.

## Acknowledgements

The authors acknowledge funding from the intramural project Modeling and Understanding SpatioTemporal Environmental INteractions project (MUSTEIN) via the Machine Learning Cluster of Excellence funded by the German Research Foundation (DFG) under the German Excellence Strategy EXC 2064/1 - 390727645. It received additional support by a fellowship within the IFI programme of the German Academic Exchange Service (DAAD). We acknowledge the International Max Planck Research School for Intelligent Systems (IMPRS-IS) for supporting Matthias Karlbauer. Martin Butz and Sebastian Otte acknowledge additional funding from the Cyber Valley in Tübingen, CyVy-RF-2020-15. The authors would also like to thank Manuel Traub, Fedor Scholz, Florian Ebmeier, Tobias Menge, Jakob Schlör, Felix Strnad, Moritz Haas, and Gwen Hirsch for invaluable discussions and feedback on the manuscript.

## References

- [1] Peter Stott. How climate change affects extreme weather events. *Science*, 352(6293):1517–1518, June 2016. doi:[10.1126/science.aaf7271](https://doi.org/10.1126/science.aaf7271).
- [2] Ben Clarke, Friederike Otto, Rupert Stuart-Smith, and Luke Harrington. Extreme weather impacts of climate change: an attribution perspective. *Environmental Research: Climate*, 1(1):012001, June 2022. ISSN 2752-5295. doi:[10.1088/2752-5295/ac6e7d](https://doi.org/10.1088/2752-5295/ac6e7d). URL <https://doi.org/10.1088/2752-5295/ac6e7d>. Publisher: IOP Publishing.
- [3] Peter Bauer, Alan Thorpe, and Gilbert Brunet. The quiet revolution of numerical weather prediction. *Nature*, 525(7567):47–55, September 2015. ISSN 1476-4687. doi:[10.1038/nature14956](https://doi.org/10.1038/nature14956). URL <https://www.nature.com/articles/nature14956>. Bandiera\_abtest: a Cg\_type: Nature Research Journals Number: 7567 Primary\_atype: Reviews Publisher: Nature Publishing Group Subject\_term: Atmospheric dynamics;Climate sciences Subject\_term\_id: atmospheric-dynamics;climate-sciences.
- [4] Peter Bauer, Peter D. Dueben, Torsten Hoefer, Tiago Quintino, Thomas C. Schulteß, and Nils P. Wedi. The digital revolution of Earth-system science. *Nature Computational Science*, 1(2):104–113, February 2021. ISSN 2662-8457. doi:[10.1038/s43588-021-00023-0](https://doi.org/10.1038/s43588-021-00023-0). URL <https://www.nature.com/articles/s43588-021-00023-0>.
- [5] Xingjian Shi, Zhourong Chen, Hao Wang, Dit-Yan Yeung, Wai-kin Wong, and Wang-chun Woo. Convolutional lstm network: A machine learning approach for precipitation nowcasting. In *Proceedings of the 28th International Conference on Neural Information Processing Systems - Volume 1*, NIPS’15, page 802–810, Cambridge, MA, USA, 2015. MIT Press.
- [6] Peter D. Dueben and Peter Bauer. Challenges and design choices for global weather and climate models based on machine learning. *Geoscientific Model Development*, 11(10):3999–4009, October 2018. ISSN 1991-9603. doi:[10.5194/gmd-11-3999-2018](https://doi.org/10.5194/gmd-11-3999-2018). URL <https://gmd.copernicus.org/articles/11/3999/2018/>.
- [7] Jonathan A. Weyn, Dale R. Durran, and Rich Caruana. Can Machines Learn to Predict Weather? Using Deep Learning to Predict Gridded 500-hPa Geopotential Height From Historical Weather Data. *Journal of Advances in Modeling Earth Systems*, 11(8):2680–2693, 2019. ISSN 1942-2466. doi:[10.1029/2019MS001705](https://doi.org/10.1029/2019MS001705). URL <https://onlinelibrary.wiley.com/doi/10.1029/2019MS001705>.
- [8] S. Scher. Toward Data-Driven Weather and Climate Forecasting: Approximating a Simple General Circulation Model With Deep Learning. *Geophysical Research Letters*, 45(22):12,616–12,622, 2018. ISSN 1944-8007. doi:[10.1029/2018GL080704](https://doi.org/10.1029/2018GL080704). URL <https://onlinelibrary.wiley.com/doi/abs/10.1029/2018GL080704>.
- [9] Yann LeCun, Yoshua Bengio, and Geoffrey Hinton. Deep learning. *Nature*, 521(7553):436–444, May 2015. ISSN 1476-4687. doi:[10.1038/nature14539](https://doi.org/10.1038/nature14539). URL <https://www.nature.com/articles/nature14539>. Number: 7553 Publisher: Nature Publishing Group.
- [10] Thorsten Kurth, Shashank Subramanian, Peter Harrington, Jaideep Pathak, Morteza Mardani, David Hall, Andrea Miele, Karthik Kashinath, and Animashree Anandkumar. FourCastNet: Accelerating Global High-Resolution Weather Forecasting using Adaptive Fourier Neural Operators, August 2022. URL [http://arxiv.org/abs/2208.05419](https://arxiv.org/abs/2208.05419) [physics]. arXiv:2208.05419 [physics].
- [11] Hans Hersbach, Bill Bell, Paul Berrisford, Shoji Hihara, András Horányi, Joaquín Muñoz-Sabater, Julien Nicolas, Carole Peubey, Raluca Radu, Dinand Schepers, Adrian Simmons, Cornel Soci, Saleh Abdalla, Xavier Abellan, Gianpaolo Balsamo, Peter Bechtold, Gionata Biavati, Jean Bidlot, Massimo Bonavita, Giovanna De Chiara, Per Dahlgren, Dick Dee, Michail Diamantakis, Rossana Dragani, Johannes Flemming, Richard Forbes, Manuel Fuentes, Alan Geer, Leo Haimberger, Sean Healy, Robin J. Hogan, Elías Hólm, Marta Janisková,

Sarah Keeley, Patrick Laloyaux, Philippe Lopez, Cristina Lupu, Gabor Radnoti, Patricia de Rosnay, Iryna Rozum, Freja Vamborg, Sébastien Villaume, and Jean-Noël Thépaut. The ERA5 global reanalysis. *Quarterly Journal of the Royal Meteorological Society*, 146(730):1999–2049, 2020. ISSN 1477-870X. doi:10.1002/qj.3803. URL <https://onlinelibrary.wiley.com/doi/abs/10.1002/qj.3803>.

[12] Stephan Rasp, Peter D. Dueben, Sebastian Scher, Jonathan A. Weyn, Soukaina Mouatadid, and Nils Thuerey. WeatherBench: A benchmark dataset for data-driven weather forecasting. *Journal of Advances in Modeling Earth Systems*, 12(11), November 2020. ISSN 1942-2466, 1942-2466. doi:10.1029/2020MS002203. URL <http://arxiv.org/abs/2002.00469>. arXiv: 2002.00469.

[13] Stephan Rasp, Michael S. Pritchard, and Pierre Gentine. Deep learning to represent subgrid processes in climate models. *Proceedings of the National Academy of Sciences*, 115(39):9684–9689, September 2018. doi:10.1073/pnas.1810286115. URL <https://www.pnas.org/doi/10.1073/pnas.1810286115>. Publisher: Proceedings of the National Academy of Sciences.

[14] Gustau Camps-Valls, Xiao Xiang Zhu, Devis Tuia, and Markus Reichstein. Introduction. In *Deep Learning for the Earth Sciences*, pages 1–11. John Wiley & Sons, Ltd, 2021. ISBN 978-1-119-64618-1. doi:10.1002/9781119646181.ch1. URL <https://onlinelibrary.wiley.com/doi/abs/10.1002/9781119646181.ch1>.

[15] Janni Yuval and Paul A. O’Gorman. Stable machine-learning parameterization of subgrid processes for climate modeling at a range of resolutions. *Nature Communications*, 11(1):3295, July 2020. ISSN 2041-1723. doi:10.1038/s41467-020-17142-3. URL <https://www.nature.com/articles/s41467-020-17142-3>. Number: 1 Publisher: Nature Publishing Group.

[16] Janni Yuval, Paul A. O’Gorman, and Chris N. Hill. Use of neural networks for stable, accurate and physically consistent parameterization of subgrid atmospheric processes with good performance at reduced precision. *Geophysical Research Letters*, 48(6), March 2021. ISSN 0094-8276, 1944-8007. doi:10.1029/2020GL091363. URL <http://arxiv.org/abs/2010.09947>. arXiv:2010.09947 [physics].

[17] Lasse Espeholt, Shreya Agrawal, Casper Sønderby, Manoj Kumar, Jonathan Heek, Carla Bromberg, Cenk Gazen, Jason Hickey, Aaron Bell, and Nal Kalchbrenner. Skillful Twelve Hour Precipitation Forecasts using Large Context Neural Networks, November 2021. URL <http://arxiv.org/abs/2111.07470>. arXiv:2111.07470 [physics].

[18] Suman Ravuri, Karel Lenc, Matthew Willson, Dmitry Kangin, Remi Lam, Piotr Mirowski, Megan Fitzsimons, Maria Athanassiadou, Sheleem Kashem, Sam Madge, Rachel Prudden, Amol Mandhane, Aidan Clark, Andrew Brock, Karen Simonyan, Raia Hadsell, Niall Robinson, Ellen Clancy, Alberto Arribas, and Shakir Mohamed. Skilful precipitation nowcasting using deep generative models of radar. *Nature*, 597(7878):672–677, September 2021. ISSN 1476-4687. doi:10.1038/s41586-021-03854-z. URL <https://doi.org/10.1038/s41586-021-03854-z>.

[19] Kaifeng Bi, Lingxi Xie, Hengheng Zhang, Xin Chen, Xiaotao Gu, and Qi Tian. Pangu-Weather: A 3D High-Resolution Model for Fast and Accurate Global Weather Forecast, November 2022. URL <http://arxiv.org/abs/2211.02556>. arXiv:2211.02556 [physics].

[20] Remi Lam, Alvaro Sanchez-Gonzalez, Matthew Willson, Peter Wirnsberger, Meire Fortunato, Alexander Pritzel, Suman Ravuri, Timo Ewalds, Ferran Alet, Zach Eaton-Rosen, Weihua Hu, Alexander Merose, Stephan Hoyer, George Holland, Jacklynn Stott, Oriol Vinyals, Shakir Mohamed, and Peter Battaglia. GraphCast: Learning skillful medium-range global weather forecasting, December 2022. URL <http://arxiv.org/abs/2212.12794>. arXiv:2212.12794 [physics].

[21] Ignacio Lopez-Gomez, Amy McGovern, Shreya Agrawal, and Jason Hickey. Global extreme heat forecasting using neural weather models. *Artificial Intelligence for the Earth Systems*, 2(1):e220035, 2023. doi:<https://doi.org/10.1175/AIES-D-22-0035.1>.

[22] Peter W. Battaglia, Jessica B. Hamrick, Victor Bapst, Alvaro Sanchez-Gonzalez, Vinicius Zambaldi, Mateusz Malinowski, Andrea Tacchetti, David Raposo, Adam Santoro, Ryan Faulkner, Caglar Gulcehre, Francis Song, Andrew Ballard, Justin Gilmer, George Dahl, Ashish Vaswani, Kelsey Allen, Charles Nash, Victoria Langston, Chris Dyer, Nicolas Heess, Daan Wierstra, Pushmeet Kohli, Matt Botvinick, Oriol Vinyals, Yujia Li, and Razvan Pascanu. Relational inductive biases, deep learning, and graph networks. *arXiv:1806.01261 [cs, stat]*, October 2018. URL <http://arxiv.org/abs/1806.01261>. arXiv: 1806.01261.

[23] Jonathan A. Weyn, Dale R. Durran, Rich Caruana, and Nathaniel Cresswell-Clay. Sub-Seasonal Forecasting With a Large Ensemble of Deep-Learning Weather Prediction Models. *Journal of Advances in Modeling Earth Systems*, 13(7):e2021MS002502, 2021. ISSN 1942-2466. doi:10.1029/2021MS002502. URL <https://agupubs.onlinelibrary.wiley.com/doi/abs/10.1029/2021MS002502>.

[24] Jaideep Pathak, Shashank Subramanian, Peter Harrington, Sanjeev Raja, Ashesh Chattopadhyay, Morteza Mardani, Thorsten Kurth, David Hall, Zongyi Li, Kamyar Azizzadenesheli, Pedram Hassanzadeh, Karthik Kashinath, and Animashree Anandkumar. FourCastNet: A Global Data-driven High-resolution Weather Model using Adaptive Fourier Neural Operators, February 2022. URL <http://arxiv.org/abs/2202.11214>. Number: arXiv:2202.11214 arXiv:2202.11214 [physics].

[25] Ryan Keisler. Forecasting Global Weather with Graph Neural Networks, February 2022. URL <http://arxiv.org/abs/2202.07575>. Number: arXiv:2202.07575 arXiv:2202.07575 [physics].

[26] Yuan Hu, Lei Chen, Zhibin Wang, and Hao Li. Swinrvnn: A data-driven ensemble forecasting model via learned distribution perturbation. *Journal of Advances in Modeling Earth Systems*, 15(2):e2022MS003211, 2023. doi:<https://doi.org/10.1029/2022MS003211>. e2022MS003211 2022MS003211.

[27] Eugenia Kalnay. Atmospheric Modeling, Data Assimilation and Predictability, November 2002. URL <https://www.cambridge.org/highereducation/books/atmospheric-modeling-data-assimilation-and-predictability/C5FD207439132836E85027754CE9BC1A>. ISBN: 9780511802270 Publisher: Cambridge University Press.

[28] Tapio Schneider, Shiwei Lan, Andrew Stuart, and João Teixeira. Earth System Modeling 2.0: A Blueprint for Models That Learn From Observations and Targeted High-Resolution Simulations. *Geophysical Research Letters*, 44(24), December 2017. ISSN 0094-8276, 1944-8007. doi:[10.1002/2017GL076101](https://doi.org/10.1002/2017GL076101). URL <http://arxiv.org/abs/1709.00037>. arXiv: 1709.00037.

[29] David J. Stensrud. *Parameterization Schemes: Keys to Understanding Numerical Weather Prediction Models*. Cambridge University Press, Cambridge, 2007. ISBN 978-0-521-12676-2. doi:[10.1017/CBO9780511812590](https://doi.org/10.1017/CBO9780511812590). URL <https://www.cambridge.org/core/books/parameterization-schemes/C7C8EC8901957314433BE7C8BC36F16D>.

[30] Julia Slingo and Tim Palmer. Uncertainty in weather and climate prediction. *Philosophical Transactions of the Royal Society A: Mathematical, Physical and Engineering Sciences*, 369(1956):4751–4767, December 2011. doi:[10.1098/rsta.2011.0161](https://doi.org/10.1098/rsta.2011.0161). URL <https://royalsocietypublishing.org/doi/10.1098/rsta.2011.0161>. Publisher: Royal Society.

[31] R. N. Bannister. A review of operational methods of variational and ensemble-variational data assimilation. *Quarterly Journal of the Royal Meteorological Society*, 143(703):607–633, 2017. ISSN 1477-870X. doi:[10.1002/qj.2982](https://doi.org/10.1002/qj.2982). URL <https://onlinelibrary.wiley.com/doi/abs/10.1002/qj.2982>.

[32] Juergen Schmidhuber. Deep Learning in Neural Networks: An Overview. *Neural Networks*, 61:85–117, January 2015. ISSN 08936080. doi:[10.1016/j.neunet.2014.09.003](https://doi.org/10.1016/j.neunet.2014.09.003). URL <http://arxiv.org/abs/1404.7828>. arXiv:1404.7828 [cs].

[33] Yoshua Bengio, Aaron Courville, and Pascal Vincent. Representation learning: a review and new perspectives. *IEEE transactions on pattern analysis and machine intelligence*, 35(8):1798–1828, August 2013. ISSN 0162-8828. doi:[10.1109/tpami.2013.50](https://doi.org/10.1109/tpami.2013.50).

[34] D.H. Wolpert and W.G. Macready. No free lunch theorems for optimization. *IEEE Transactions on Evolutionary Computation*, 1(1):67–82, 1997. doi:[10.1109/4235.585893](https://doi.org/10.1109/4235.585893).

[35] D.H. Wolpert and W.G. Macready. No free lunch theorems for optimization. *IEEE Transactions on Evolutionary Computation*, 1(1):67–82, April 1997. ISSN 1941-0026. doi:[10.1109/4235.585893](https://doi.org/10.1109/4235.585893). Conference Name: IEEE Transactions on Evolutionary Computation.

[36] Daniel Harris, Efi Foufoula-Georgiou, Kelvin K. Droegemeier, and Jason J. Levit. Multiscale Statistical Properties of a High-Resolution Precipitation Forecast. *Journal of Hydrometeorology*, 2(4):406–418, August 2001. ISSN 1525-755X, 1525-7541. doi:[10.1175/1525-7541\(2001\)002<0406:MSPOAH>2.0.CO;2](https://doi.org/10.1175/1525-7541(2001)002<0406:MSPOAH>2.0.CO;2). URL [http://journals.ametsoc.org/doi/10.1175/1525-7541\(2001\)002<0406:MSPOAH>2.0.CO;2](http://journals.ametsoc.org/doi/10.1175/1525-7541(2001)002<0406:MSPOAH>2.0.CO;2).

[37] Travis M. Smith, Valliappa Lakshmanan, Gregory J. Stumpf, Kiel L. Ortega, Kurt Hondl, Karen Cooper, Kristin M. Calhoun, Darrel M. Kingfield, Kevin L. Manross, Robert Toomey, and Jeff Brogden. Multi-Radar Multi-Sensor (MRMS) Severe Weather and Aviation Products: Initial Operating Capabilities. *Bulletin of the American Meteorological Society*, 97(9):1617–1630, September 2016. ISSN 0003-0007, 1520-0477. doi:[10.1175/BAMS-D-14-00173.1](https://doi.org/10.1175/BAMS-D-14-00173.1). URL <https://journals.ametsoc.org/view/journals/bams/97/9/bams-d-14-00173.1.xml>. Publisher: American Meteorological Society Section: Bulletin of the American Meteorological Society.

[38] Kenneth P. Bowman and Cameron R. Homeyer. GridRad - Three-Dimensional Gridded NEXRAD WSR-88D Radar Data, 2017. URL <https://rda.ucar.edu/datasets/ds841.0/>.

[39] Gary K. Davis. History of the NOAA satellite program. *Journal of Applied Remote Sensing*, 1(1):012504, January 2007. ISSN 1931-3195, 1931-3195. doi:10.1117/1.2642347. URL <https://www.spiedigitallibrary.org/journals/journal-of-applied-remote-sensing/volume-1/issue-1/012504/History-of-the-NOAA-satellite-program/10.1117/1.2642347.full>. Publisher: SPIE.

[40] J. Schulz, P. Albert, H.-D. Behr, D. Caprion, H. Deneke, S. Dewitte, B. Dürr, P. Fuchs, A. Gratzki, P. Hechler, R. Hollmann, S. Johnston, K.-G. Karlsson, T. Manninen, R. Müller, M. Reuter, A. Riihelä, R. Roebeling, N. Selbach, A. Tetzlaff, W. Thomas, M. Werscheck, E. Wolters, and A. Zelenka. Operational climate monitoring from space: the EUMETSAT Satellite Application Facility on Climate Monitoring (CM-SAF). *Atmospheric Chemistry and Physics*, 9(5):1687–1709, March 2009. ISSN 1680-7316. doi:10.5194/acp-9-1687-2009. URL <https://acp.copernicus.org/articles/9/1687/2009/>. Publisher: Copernicus GmbH.

[41] Urs Germann and Isztar Zawadzki. Scale Dependence of the Predictability of Precipitation from Continental Radar Images. Part II: Probability Forecasts. *Journal of Applied Meteorology and Climatology*, 43(1):74–89, January 2004. ISSN 1520-0450, 0894-8763. doi:10.1175/1520-0450(2004)043<0074:SDOTPO>2.0.CO;2. URL [https://journals.ametsoc.org/view/journals/apme/43/1/1520-0450\\_2004\\_043\\_0074\\_sdotp\\_2.0.co\\_2.xml](https://journals.ametsoc.org/view/journals/apme/43/1/1520-0450_2004_043_0074_sdotp_2.0.co_2.xml). Publisher: American Meteorological Society Section: Journal of Applied Meteorology and Climatology.

[42] Jun-Ichi Yano, Michał Z. Ziemiański, Mike Cullen, Piet Termonia, Jeanette Onvlee, Lisa Bengtsson, Alberto Carrassi, Richard Davy, Anna Deluca, Suzanne L. Gray, Víctor Homar, Martin Köhler, Simon Krichak, Silas Michaelides, Vaughan T. J. Phillips, Pedro M. M. Soares, and Andrzej A. Wyszogrodzki. Scientific Challenges of Convective-Scale Numerical Weather Prediction. *Bulletin of the American Meteorological Society*, 99(4):699–710, April 2018. ISSN 0003-0007, 1520-0477. doi:10.1175/BAMS-D-17-0125.1. URL <https://journals.ametsoc.org/view/journals/bams/99/4/bams-d-17-0125.1.xml>. Publisher: American Meteorological Society Section: Bulletin of the American Meteorological Society.

[43] A. T. Karpachev and N. A. Gasilov. Zonal and meridional wind components derived from intercosmos-19 hmF2 measurements. *Advances in Space Research*, 27(6):1245–1252, January 2001. ISSN 0273-1177. doi:10.1016/S0273-1177(01)00170-3. URL <https://www.sciencedirect.com/science/article/pii/S0273117701001703>.

[44] Sagar Garg, Stephan Rasp, and Nils Thuerey. WeatherBench Probability: A benchmark dataset for probabilistic medium-range weather forecasting along with deep learning baseline models, May 2022. URL <http://arxiv.org/abs/2205.00865>. arXiv:2205.00865 [physics].

[45] Christian Körner. The use of ‘altitude’ in ecological research. *Trends in ecology & evolution*, 22(11):569–574, 2007.

[46] Sebastian U Senger. Meteorologisch-klimatologisches grundwissen eine einführung mit übungen, aufgaben und lösungenautoren: Ewald zmarsly, wilhelm kuttler, hermann pethe, 1999.

[47] Roland B Stull, C Donald Ahrens, et al. *Meteorology for scientists and engineers*. Brooks/Cole, 2000.

[48] Mustafa Cavcar. The international standard atmosphere (isa). *Anadolu University, Turkey*, 30(9):1–6, 2000.

[49] Stephan Rasp and Nils Thuerey. Data-Driven Medium-Range Weather Prediction With a Resnet Pretrained on Climate Simulations: A New Model for WeatherBench. *Journal of Advances in Modeling Earth Systems*, 13(2):e2020MS002405, 2021. ISSN 1942-2466. doi:10.1029/2020MS002405. URL <https://onlinelibrary.wiley.com/doi/abs/10.1029/2020MS002405>.

[50] Jeffrey L. Elman. Distributed representations, simple recurrent networks, and grammatical structure. *Machine Learning*, 7(2-3):195–225, September 1991. ISSN 0885-6125, 1573-0565. doi:10.1007/BF00114844.

[51] Samy Bengio, Oriol Vinyals, Navdeep Jaitly, and Noam Shazeer. Scheduled sampling for sequence prediction with recurrent neural networks. In *Proceedings of the 28th International Conference on Neural Information Processing Systems - Volume 1*, NIPS’15, pages 1171–1179, Cambridge, MA, USA, 2015. MIT Press.

[52] Alex M Lamb, Anirudh Goyal ALIAS PARTH GOYAL, Ying Zhang, Saizheng Zhang, Aaron C Courville, and Yoshua Bengio. Professor Forcing: A New Algorithm for Training Recurrent Networks. In *Advances in Neural Information Processing Systems*, volume 29. Curran Associates, Inc., 2016. URL <https://proceedings.neurips.cc/paper/2016/hash/16026d60ff9b54410b3435b403af226-Abstract.html>.

[53] Y. Bengio, P. Simard, and P. Frasconi. Learning long-term dependencies with gradient descent is difficult. *IEEE Transactions on Neural Networks*, 5(2):157–166, March 1994. ISSN 1941-0093. doi:10.1109/72.279181. Conference Name: IEEE Transactions on Neural Networks.

[54] Razvan Pascanu, Tomas Mikolov, and Yoshua Bengio. On the difficulty of training recurrent neural networks. In *Proceedings of the 30th International Conference on International Conference on Machine Learning - Volume 28*, ICML'13, page III–1310–III–1318. JMLR.org, 2013.

[55] Sepp Hochreiter and Jürgen Schmidhuber. Long Short-Term Memory. *Neural Computation*, 9(8):1735–1780, November 1997. ISSN 0899-7667. doi:10.1162/neco.1997.9.8.1735. URL <https://doi.org/10.1162/neco.1997.9.8.1735>.

[56] Corentin Tallec and Yann Ollivier. Can recurrent neural networks warp time? In *International Conference on Learning Representations*, 2018.

[57] Razvan Pascanu, Tomas Mikolov, and Yoshua Bengio. On the difficulty of training recurrent neural networks. In *Proceedings of the 30th International Conference on International Conference on Machine Learning - Volume 28*, ICML'13, page III–1310–III–1318. JMLR.org, 2013.

[58] Luke Metz, C. Daniel Freeman, Samuel S. Schoenholz, and Tal Kachman. Gradients are Not All You Need, January 2022. URL <http://arxiv.org/abs/2111.05803>. Number: arXiv:2111.05803 arXiv:2111.05803 [cs, stat].

[59] Joost van Amersfoort, Anitha Kannan, Marc’Aurelio Ranzato, Arthur Szlam, Du Tran, and Soumith Chintala. Transformation-Based Models of Video Sequences. *arXiv:1701.08435 [cs]*, April 2017. URL <http://arxiv.org/abs/1701.08435>. arXiv: 1701.08435.

[60] Pauline Luc, Aidan Clark, Sander Dieleman, Diego de Las Casas, Yotam Doron, Albin Cassirer, and Karen Simonyan. Transformation-based Adversarial Video Prediction on Large-Scale Data. *arXiv:2003.04035 [cs]*, December 2020. URL <http://arxiv.org/abs/2003.04035>. arXiv: 2003.04035.

[61] Casper Kaae Sønderby, Lasse Espeholt, Jonathan Heek, Mostafa Dehghani, Avital Oliver, Tim Salimans, Shreya Agrawal, Jason Hickey, and Nal Kalchbrenner. MetNet: A Neural Weather Model for Precipitation Forecasting. *arXiv:2003.12140 [physics, stat]*, March 2020. URL <http://arxiv.org/abs/2003.12140>. arXiv: 2003.12140.

[62] Tim Palmer. The ECMWF ensemble prediction system: Looking back (more than) 25 years and projecting forward 25 years. *Quarterly Journal of the Royal Meteorological Society*, 145(S1):12–24, 2019. ISSN 1477-870X. doi:10.1002/qj.3383. URL <https://onlinelibrary.wiley.com/doi/abs/10.1002/qj.3383>.

[63] Sam Bond-Taylor, Adam Leach, Yang Long, and Chris G. Willcocks. Deep Generative Modelling: A Comparative Review of VAEs, GANs, Normalizing Flows, Energy-Based and Autoregressive Models. *IEEE Transactions on Pattern Analysis and Machine Intelligence*, pages 1–1, 2021. ISSN 0162-8828, 2160-9292, 1939-3539. doi:10.1109/TPAMI.2021.3116668. URL <http://arxiv.org/abs/2103.04922>. arXiv: 2103.04922.

[64] Danilo Jimenez Rezende, Shakir Mohamed, and Daan Wierstra. Stochastic backpropagation and approximate inference in deep generative models. In *Proceedings of the 31st International Conference on International Conference on Machine Learning - Volume 32*, ICML'14, page II–1278–II–1286. JMLR.org, 2014.

[65] Diederik P. Kingma and Max Welling. Auto-encoding variational bayes. In *International Conference on Learning Representations*, 2014.

[66] Ian Goodfellow, Jean Pouget-Abadie, Mehdi Mirza, Bing Xu, David Warde-Farley, Sherjil Ozair, Aaron Courville, and Yoshua Bengio. Generative adversarial nets. In Z. Ghahramani, M. Welling, C. Cortes, N. Lawrence, and K.Q. Weinberger, editors, *Advances in Neural Information Processing Systems*, volume 27. Curran Associates, Inc., 2014.

[67] Danilo Rezende and Shakir Mohamed. Variational inference with normalizing flows. In Francis Bach and David Blei, editors, *Proceedings of the 32nd International Conference on Machine Learning*, volume 37 of *Proceedings of Machine Learning Research*, pages 1530–1538, Lille, France, 07–09 Jul 2015. PMLR. URL <https://proceedings.mlr.press/v37/rezende15.html>.

[68] I. Kobyzev, S. D. Prince, and M. A. Brubaker. Normalizing flows: An introduction and review of current methods. *IEEE Transactions on Pattern Analysis & Machine Intelligence*, 43(11):3964–3979, nov 2021. ISSN 1939-3539. doi:10.1109/TPAMI.2020.2992934.

[69] Jonathan Ho, Ajay Jain, and Pieter Abbeel. Denoising diffusion probabilistic models. In H. Larochelle, M. Ranzato, R. Hadsell, M.F. Balcan, and H. Lin, editors, *Advances in Neural Information Processing Systems*, volume 33, pages 6840–6851. Curran Associates, Inc., 2020. URL [https://proceedings.neurips.cc/paper\\_files/paper/2020/file/4c5bcfec8584af0d967f1ab10179ca4b-Paper.pdf](https://proceedings.neurips.cc/paper_files/paper/2020/file/4c5bcfec8584af0d967f1ab10179ca4b-Paper.pdf).

[70] Emily Denton and Rob Fergus. Stochastic video generation with a learned prior. In Jennifer Dy and Andreas Krause, editors, *Proceedings of the 35th International Conference on Machine Learning*, volume 80 of *Proceedings of Machine Learning Research*, pages 1174–1183. PMLR, 10–15 Jul 2018.

[71] Mohammad Babaeizadeh, Chelsea Finn, Dumitru Erhan, Roy H. Campbell, and Sergey Levine. Stochastic variational video prediction. In *International Conference on Learning Representations*, 2018.

[72] Aidan Clark, Jeff Donahue, and Karen Simonyan. Adversarial Video Generation on Complex Datasets, September 2019. URL <http://arxiv.org/abs/1907.06571>. arXiv:1907.06571 [cs, stat].

[73] Jussi Leinonen, Daniele Nerini, and Alexis Berne. Stochastic Super-Resolution for Downscaling Time-Evolving Atmospheric Fields with a Generative Adversarial Network. *IEEE Transactions on Geoscience and Remote Sensing*, 59(9):7211–7223, September 2021. ISSN 0196-2892, 1558-0644. doi:10.1109/TGRS.2020.3032790. URL <http://arxiv.org/abs/2005.10374>. arXiv:2005.10374 [physics, stat].

[74] Chen, Zhang, Liu, and Zeng. Generative Adversarial Networks Capabilities for Super-Resolution Reconstruction of Weather Radar Echo Images. *Atmosphere*, 10(9):555, September 2019. ISSN 2073-4433. doi:10.3390/atmos10090555. URL <https://www.mdpi.com/2073-4433/10/9/555>.

[75] Bing Gong, Michael Langguth, Yan Ji, Amirpasha Mozaffari, Scarlet Stadtler, Karim Mache, and Martin G. Schultz. Temperature forecasting by deep learning methods. preprint, Climate and Earth system modeling, March 2022. URL <https://gmd.copernicus.org/preprints/gmd-2021-430/>.

[76] Ilan Price and Stephan Rasp. Increasing the accuracy and resolution of precipitation forecasts using deep generative models. In *International Conference on Artificial Intelligence and Statistics, AISTATS 2022, 28-30 March 2022, Virtual Event*, volume 151 of *Proceedings of Machine Learning Research*, pages 10555–10571. PMLR, 2022.

[77] Konstantin Klemmer, Sudipan Saha, Matthias Kahl, Tianlin Xu, and Xiao Xiang Zhu. Generative modeling of spatio-temporal weather patterns with extreme event conditioning. *arXiv:2104.12469 [physics]*, April 2021. URL <http://arxiv.org/abs/2104.12469>. arXiv: 2104.12469.

[78] Laurent Girin, Simon Leglaive, Xiaoyu Bie, Julien Diard, Thomas Hueber, and Xavier Alameda-Pineda. Dynamical Variational Autoencoders: A Comprehensive Review. *Foundations and Trends® in Machine Learning*, 15(1-2):1–175, 2021. ISSN 1935-8237, 1935-8245. doi:10.1561/2200000089. URL <http://arxiv.org/abs/2008.12595>. arXiv: 2008.12595.

[79] Danijar Hafner, Timothy Lillicrap, Jimmy Ba, and Mohammad Norouzi. Dream to control: Learning behaviors by latent imagination. In *International Conference on Learning Representations*, 2020.

[80] Danijar Hafner, Timothy P Lillicrap, Mohammad Norouzi, and Jimmy Ba. Mastering atari with discrete world models. In *International Conference on Learning Representations*, 2021.

[81] Christopher M. Bishop. *Pattern recognition and machine learning*. Information science and statistics. Springer, New York, 2006. ISBN 978-0-387-31073-2.

[82] Xingjian Shi, Zhihan Gao, Leonard Lausen, Hao Wang, Dit-Yan Yeung, Wai-kin Wong, and Wang-chun Woo. Deep learning for precipitation nowcasting: A benchmark and a new model. In *Proceedings of the 31st International Conference on Neural Information Processing Systems, NIPS’17*, page 5622–5632, Red Hook, NY, USA, 2017. Curran Associates Inc. ISBN 9781510860964.

[83] Sylwester Klocek, Haiyu Dong, Matthew Dixon, Panashe Kanengoni, Najeeb Kazmi, Pete Luferenko, Zhongjian Lv, Shikhar Sharma, Jonathan Weyn, and Siqi Xiang. MS-nowcasting: Operational Precipitation Nowcasting with Convolutional LSTMs at Microsoft Weather, May 2022. URL <http://arxiv.org/abs/2111.09954>. Number: arXiv:2111.09954 arXiv:2111.09954 [physics].

[84] Georgy Ayzel, Tobias Scheffer, and Maik Heistermann. RainNet v1.0: a convolutional neural network for radar-based precipitation nowcasting. *Geoscientific Model Development*, 13(6):2631–2644, June 2020. ISSN 1991-959X. doi:10.5194/gmd-13-2631-2020. URL <https://gmd.copernicus.org/articles/13/2631/2020/>. Publisher: Copernicus GmbH.

[85] Eric Gilleland, David Ahijevych, Barbara G. Brown, Barbara Casati, and Elizabeth E. Ebert. Intercomparison of Spatial Forecast Verification Methods. *Weather and Forecasting*, 24(5):1416–1430, October 2009. ISSN 1520-0434, 0882-8156. doi:10.1175/2009WAF2222269.1. URL [https://journals.ametsoc.org/view/journals/wefo/24/5/2009waf2222269\\_1.xml](https://journals.ametsoc.org/view/journals/wefo/24/5/2009waf2222269_1.xml). Publisher: American Meteorological Society Section: Weather and Forecasting.

[86] Adrian G. Barnett, Jolieke C. van der Pols, and Annette J. Dobson. Regression to the mean: what it is and how to deal with it. *International Journal of Epidemiology*, 34(1):215–220, February 2005. ISSN 0300-5771. doi:10.1093/ije/dyh299.

[87] Michaël Mathieu, Camille Couprie, and Yann LeCun. Deep multi-scale video prediction beyond mean square error. In Yoshua Bengio and Yann LeCun, editors, *International Conference on Learning Representations*, 2016.

[88] Andre Graubner, Kamyar Kamyar Azizzadenesheli, Jaideep Pathak, Morteza Mardani, Mike Pritchard, Karthik Kashinath, and Anima Anandkumar. Calibration of large neural weather models. In *NeurIPS 2022 Workshop on Tackling Climate Change with Machine Learning*, 2022.

[89] Sebastian Scher and Gabriele Messori. Ensemble Methods for Neural Network-Based Weather Forecasts. *Journal of Advances in Modeling Earth Systems*, 13(2), 2021. ISSN 1942-2466. doi:[10.1029/2020MS002331](https://doi.org/10.1029/2020MS002331). URL <https://onlinelibrary.wiley.com/doi/abs/10.1029/2020MS002331>.

[90] Alex Kendall and Yarin Gal. What uncertainties do we need in bayesian deep learning for computer vision? In *Advances in Neural Information Processing Systems*, volume 30. Curran Associates, Inc., 2017.

[91] Andrew Stirn and David A. Knowles. Variational Variance: Simple, Reliable, Calibrated Heteroscedastic Noise Variance Parameterization, October 2020. URL <http://arxiv.org/abs/2006.04910>. arXiv:2006.04910 [cs, stat].

[92] Maximilian Seitzer, Arash Tavakoli, Dimitrije Antic, and Georg Martius. On the pitfalls of heteroscedastic uncertainty estimation with probabilistic neural networks. In *International Conference on Learning Representations*, 2022.

[93] Partha Ghosh, Mehdi S. M. Sajjadi, Antonio Vergari, Michael Black, and Bernhard Scholkopf. From variational to deterministic autoencoders. In *International Conference on Learning Representations*, 2020.

[94] Tilman Gneiting and Adrian E Raftery. Strictly proper scoring rules, prediction, and estimation. *Journal of the American Statistical Association*, 102(477):359–378, 2007. doi:[10.1198/016214506000001437](https://doi.org/10.1198/016214506000001437).

[95] Jonathan Berrisch and Florian Ziel. Crps learning. *Journal of Econometrics*, 2021. ISSN 0304-4076. doi:<https://doi.org/10.1016/j.jeconom.2021.11.008>.

[96] Stephan Rasp and Sebastian Lerch. Neural networks for postprocessing ensemble weather forecasts. *Monthly Weather Review*, 146(11):3885–3900, 2018. doi:<https://doi.org/10.1175/MWR-D-18-0187.1>.

[97] William E. Chapman, Luca Delle Monache, Stefano Alessandrini, Aneesh C. Subramanian, F. Martin Ralph, Shang-Ping Xie, Sebastian Lerch, and Negin Hayatbini. Probabilistic predictions from deterministic atmospheric river forecasts with deep learning. *Monthly Weather Review*, 150(1):215–234, 2022. doi:<https://doi.org/10.1175/MWR-D-21-0106.1>.

[98] Zhou Wang, A.C. Bovik, H.R. Sheikh, and E.P. Simoncelli. Image quality assessment: from error visibility to structural similarity. *IEEE Transactions on Image Processing*, 13(4):600–612, April 2004. ISSN 1941-0042. doi:[10.1109/TIP.2003.819861](https://doi.org/10.1109/TIP.2003.819861). Conference Name: IEEE Transactions on Image Processing.

[99] Zhou Wang and Alan C. Bovik. Mean squared error: Love it or leave it? A new look at Signal Fidelity Measures. *IEEE Signal Processing Magazine*, 26(1):98–117, January 2009. ISSN 1558-0792. doi:[10.1109/MSP.2008.930649](https://doi.org/10.1109/MSP.2008.930649). Conference Name: IEEE Signal Processing Magazine.

[100] Nigel M. Roberts and Humphrey W. Lean. Scale-Selective Verification of Rainfall Accumulations from High-Resolution Forecasts of Convective Events. *Monthly Weather Review*, 136(1):78–97, January 2008. ISSN 1520-0493, 0027-0644. doi:[10.1175/2007MWR2123.1](https://doi.org/10.1175/2007MWR2123.1). URL <https://journals.ametsoc.org/view/journals/mwre/136/1/2007mwr2123.1.xml>. Publisher: American Meteorological Society Section: Monthly Weather Review.

[101] Jian Zhang, Peter F. Craigmile, and Noel Cressie. Loss Function Approaches to Predict a Spatial Quantile and Its Exceedance Region. *Technometrics*, 50(2):216–227, May 2008. ISSN 0040-1706. doi:[10.1198/004017008000000226](https://doi.org/10.1198/004017008000000226). URL <https://doi.org/10.1198/004017008000000226>.

[102] Jake Snell, Karl Ridgeway, Renjie Liao, Brett D. Roads, Michael C. Mozer, and Richard S. Zemel. Learning to generate images with perceptual similarity metrics. In *2017 IEEE International Conference on Image Processing (ICIP)*, pages 4277–4281, September 2017. doi:[10.1109/ICIP.2017.8297089](https://doi.org/10.1109/ICIP.2017.8297089). ISSN: 2381-8549.

[103] Johannes Gensheimer, Alexander J. Turner, Philipp Köhler, Christian Frankenberg, and Jia Chen. A convolutional neural network for spatial downscaling of satellite-based solar-induced chlorophyll fluorescence (SIFnet). *Biogeosciences*, 19(6):1777–1793, March 2022. ISSN 1726-4170. doi:[10.5194/bg-19-1777-2022](https://doi.org/10.5194/bg-19-1777-2022). URL <https://bg.copernicus.org/articles/19/1777/2022/>. Publisher: Copernicus GmbH.

[104] Ryan Lagerquist and Imme Ebert-Uphoff. Can We Integrate Spatial Verification Methods into Neural Network Loss Functions for Atmospheric Science? *Artificial Intelligence for the Earth Systems*, 1(4):e220021, October 2022. ISSN 2769-7525. doi:[10.1175/AIES-D-22-0021.1](https://doi.org/10.1175/AIES-D-22-0021.1). URL <https://journals.ametsoc.org/view/journals/aies/1/4/AIES-D-22-0021.1.xml>.

[105] Aaron van den Oord, Yazhe Li, and Oriol Vinyals. Representation Learning with Contrastive Predictive Coding, January 2019. URL <http://arxiv.org/abs/1807.03748>. arXiv:1807.03748 [cs, stat].

[106] Ming Chen, Zhewei Wei, Zengfeng Huang, Bolin Ding, and Yaliang Li. Simple and deep graph convolutional networks. In Hal Daumé III and Aarti Singh, editors, *Proceedings of the 37th International Conference on Machine Learning*, volume 119 of *Proceedings of Machine Learning Research*, pages 1725–1735. PMLR, 13–18 Jul 2020.

[107] Xiaolong Wang and Abhinav Gupta. Unsupervised learning of visual representations using videos. In *2015 IEEE International Conference on Computer Vision, ICCV 2015, Santiago, Chile, December 7-13, 2015*, pages 2794–2802. IEEE Computer Society, 2015. doi:[10.1109/ICCV.2015.320](https://doi.org/10.1109/ICCV.2015.320).

[108] Karen Stengel, Andrew Glaws, Dylan Hettinger, and Ryan N. King. Adversarial super-resolution of climatological wind and solar data. *Proceedings of the National Academy of Sciences*, 117(29):16805–16815, July 2020. doi:[10.1073/pnas.1918964117](https://doi.org/10.1073/pnas.1918964117). URL <https://www.pnas.org/doi/full/10.1073/pnas.1918964117>. Publisher: Proceedings of the National Academy of Sciences.

[109] Sebastian Hoffmann and Christian Lessig. Atmodist: Self-supervised representation learning for atmospheric dynamics. *Environmental Data Science*, 2:e6, 2023. doi:[10.1017/eds.2023.1](https://doi.org/10.1017/eds.2023.1).

[110] Kevin Sahr, Denis White, and A. Jon Kimerling. Geodesic discrete global grid systems. *Cartography and Geographic Information Science*, 30(2):121–134, 2003. doi:[10.1559/152304003100011090](https://doi.org/10.1559/152304003100011090).

[111] Alexey Dosovitskiy, Lucas Beyer, Alexander Kolesnikov, Dirk Weissenborn, Xiaohua Zhai, Thomas Unterthiner, Mostafa Dehghani, Matthias Minderer, Georg Heigold, Sylvain Gelly, Jakob Uszkoreit, and Neil Houlsby. An image is worth 16x16 words: Transformers for image recognition at scale. In *International Conference on Learning Representations*, 2021.

[112] Olaf Ronneberger, Philipp Fischer, and Thomas Brox. U-net: Convolutional networks for biomedical image segmentation. In Nassir Navab, Joachim Hornegger, William M. Wells, and Alejandro F. Frangi, editors, *Medical Image Computing and Computer-Assisted Intervention – MICCAI 2015*, pages 234–241, Cham, 2015. Springer International Publishing. ISBN 978-3-319-24574-4.

[113] A. Vaswani, P. Ramachandran, A. Srinivas, N. Parmar, B. Hechtman, and J. Shlens. Scaling local self-attention for parameter efficient visual backbones. In *2021 IEEE/CVF Conference on Computer Vision and Pattern Recognition (CVPR)*, pages 12889–12899, Los Alamitos, CA, USA, jun 2021. IEEE Computer Society. doi:[10.1109/CVPR46437.2021.01270](https://doi.org/10.1109/CVPR46437.2021.01270).

[114] Huimin Huang, Lanfen Lin, Ruofeng Tong, Hongjie Hu, Qiaowei Zhang, Yutaro Iwamoto, Xianhua Han, Yen-Wei Chen, and Jian Wu. UNet 3+: A Full-Scale Connected UNet for Medical Image Segmentation. In *ICASSP 2020 - 2020 IEEE International Conference on Acoustics, Speech and Signal Processing (ICASSP)*, pages 1055–1059, Barcelona, Spain, May 2020. IEEE. ISBN 978-1-5090-6631-5. doi:[10.1109/ICASSP40776.2020.9053405](https://doi.org/10.1109/ICASSP40776.2020.9053405). URL <https://ieeexplore.ieee.org/document/9053405/>.

[115] Haoqi Fan, Bo Xiong, Karttikeya Mangalam, Yanghao Li, Zhicheng Yan, Jitendra Malik, and Christoph Feichtenhofer. Multiscale Vision Transformers, April 2021. URL [http://arxiv.org/abs/2104.11227](https://arxiv.org/abs/2104.11227). arXiv:2104.11227 [cs].

[116] Ryan Lagerquist, David Turner, Imme Ebert-Uphoff, Jebb Stewart, and Venita Hagerty. Using Deep Learning to Emulate and Accelerate a Radiative Transfer Model. *Journal of Atmospheric and Oceanic Technology*, 38(10):1673–1696, October 2021. ISSN 0739-0572, 1520-0426. doi:[10.1175/JTECH-D-21-0007.1](https://doi.org/10.1175/JTECH-D-21-0007.1). URL <https://journals.ametsoc.org/view/journals/atot/38/10/JTECH-D-21-0007.1.xml>. Publisher: American Meteorological Society Section: Journal of Atmospheric and Oceanic Technology.

[117] Rilwan A. Adewoyin, Peter Dueben, Peter Watson, Yulan He, and Ritabrata Dutta. TRU-NET: a deep learning approach to high resolution prediction of rainfall. *Machine Learning*, 110(8):2035–2062, August 2021. ISSN 0885-6125, 1573-0565. doi:[10.1007/s10994-021-06022-6](https://doi.org/10.1007/s10994-021-06022-6).

[118] Kevin Trebing, Tomasz Stanczyk, and Siamak Mehrkanoon. Smaat-unet: Precipitation nowcasting using a small attention-unet architecture. *Pattern Recognition Letters*, 145:178–186, 2021. ISSN 0167-8655. doi:<https://doi.org/10.1016/j.patrec.2021.01.036>.

[119] Shreya Agrawal, Luke Barrington, Carla Bromberg, John Burge, Cenk Gazen, and Jason Hickey. Machine Learning for Precipitation Nowcasting from Radar Images. *arXiv:1912.12132 [cs, stat]*, December 2019. URL [http://arxiv.org/abs/1912.12132](https://arxiv.org/abs/1912.12132). arXiv: 1912.12132.

[120] Selim Furkan Tekin, Oguzhan Karaahmetoglu, Fatih Ilhan, Ismail Balaban, and Suleyman Serdar Kozat. Spatio-temporal Weather Forecasting and Attention Mechanism on Convolutional LSTMs, February 2021. URL [http://arxiv.org/abs/2102.00696](https://arxiv.org/abs/2102.00696). arXiv:2102.00696 [cs].

[121] Jonathan A. Weyn, Dale R. Durran, and Rich Caruana. Improving Data-Driven Global Weather Prediction Using Deep Convolutional Neural Networks on a Cubed Sphere. *Journal of Advances in Modeling Earth Systems*, 12

(9):e2020MS002109, 2020. ISSN 1942-2466. doi:[10.1029/2020MS002109](https://doi.org/10.1029/2020MS002109). URL <https://onlinelibrary.wiley.com/doi/abs/10.1029/2020MS002109>.

[122] Ilya Sutskever, Oriol Vinyals, and Quoc V. Le. Sequence to Sequence Learning with Neural Networks, December 2014. URL <http://arxiv.org/abs/1409.3215>. arXiv:1409.3215 [cs].

[123] Kyunghyun Cho, Bart van Merriënboer, Dzmitry Bahdanau, and Yoshua Bengio. On the Properties of Neural Machine Translation: Encoder-Decoder Approaches, October 2014. URL <http://arxiv.org/abs/1409.1259>. arXiv:1409.1259 [cs, stat].

[124] Kyunghyun Cho, Bart van Merriënboer, Caglar Gulcehre, Dzmitry Bahdanau, Fethi Bougares, Holger Schwenk, and Yoshua Bengio. Learning phrase representations using RNN encoder–decoder for statistical machine translation. In *Proceedings of the 2014 Conference on Empirical Methods in Natural Language Processing (EMNLP)*, pages 1724–1734, Doha, Qatar, October 2014. Association for Computational Linguistics. doi:[10.3115/v1/D14-1179](https://doi.org/10.3115/v1/D14-1179).

[125] Christian Gumbsch, Martin V. Butz, and Georg Martius. Sparsely changing latent states for prediction and planning in partially observable domains. In *Advances in Neural Information Processing Systems*, 2021.

[126] Ashish Vaswani, Noam Shazeer, Niki Parmar, Jakob Uszkoreit, Llion Jones, Aidan N Gomez, Łukasz Kaiser, and Illia Polosukhin. Attention is all you need. In *Advances in Neural Information Processing Systems*, volume 30. Curran Associates, Inc., 2017.

[127] Angelos Katharopoulos, Apoorv Vyas, Nikolaos Pappas, and François Fleuret. Transformers are RNNs: Fast Autoregressive Transformers with Linear Attention. *arXiv:2006.16236 [cs, stat]*, August 2020. URL <http://arxiv.org/abs/2006.16236>. arXiv: 2006.16236.

[128] Zhong Li, Haotian Jiang, and Qianxiao Li. On the approximation properties of recurrent encoder-decoder architectures. In *International Conference on Learning Representations*, 2022.

[129] Edward N. Lorenz. The predictability of a flow which possesses many scales of motion. *Tellus*, 21(3):289–307, 1969. ISSN 2153-3490. doi:[10.1111/j.2153-3490.1969.tb00444.x](https://doi.org/10.1111/j.2153-3490.1969.tb00444.x). URL <https://onlinelibrary.wiley.com/doi/abs/10.1111/j.2153-3490.1969.tb00444.x>.

[130] S. Lovejoy and D. Schertzer. Generalized Scale Invariance in the Atmosphere and Fractal Models of Rain. *Water Resources Research*, 21(8):1233–1250, August 1985. ISSN 00431397. doi:[10.1029/WR021i008p01233](https://doi.org/10.1029/WR021i008p01233). URL <http://doi.wiley.com/10.1029/WR021i008p01233>.

[131] Richard Courant, Kurt Friedrichs, and Hans Lewy. Über die partiellen differenzengleichungen der mathematischen physik. *Mathematische annalen*, 100(1):32–74, 1928.

[132] Yann Lecun and Yoshua Bengio. Convolutional Networks for Images, Speech and Time Series. In Michael A. Arbib, editor, *The Handbook of Brain Theory and Neural Networks*, pages 255–258. The MIT Press, 1995.

[133] Fisher Yu and Vladlen Koltun. Multi-scale context aggregation by dilated convolutions. In *International Conference on Learning Representations*, 2016.

[134] Z. Liu, Y. Lin, Y. Cao, H. Hu, Y. Wei, Z. Zhang, S. Lin, and B. Guo. Swin transformer: Hierarchical vision transformer using shifted windows. In *2021 IEEE/CVF International Conference on Computer Vision (ICCV)*, pages 9992–10002, Los Alamitos, CA, USA, oct 2021. IEEE Computer Society. doi:[10.1109/ICCV48922.2021.00986](https://doi.org/10.1109/ICCV48922.2021.00986).

[135] Yi Tay, Mostafa Dehghani, Dara Bahri, and Donald Metzler. Efficient transformers: A survey. *ACM Comput. Surv.*, 55(6), dec 2022. ISSN 0360-0300. doi:[10.1145/3530811](https://doi.org/10.1145/3530811).

[136] Zongyi Li, Daniel Zhengyu Huang, Burigede Liu, and Anima Anandkumar. Fourier Neural Operator with Learned Deformations for PDEs on General Geometries, July 2022. URL <http://arxiv.org/abs/2207.05209>. arXiv:2207.05209 [cs, math].

[137] John Guibas, Morteza Mardani, Zongyi Li, Andrew Tao, Anima Anandkumar, and Bryan Catanzaro. Efficient token mixing for transformers via adaptive fourier neural operators. In *International Conference on Learning Representations*, 2022.

[138] Michael M. Bronstein, Joan Bruna, Taco Cohen, and Petar Veličković. Geometric Deep Learning: Grids, Groups, Graphs, Geodesics, and Gauges, May 2021. URL <http://arxiv.org/abs/2104.13478>. arXiv:2104.13478 [cs, stat].

[139] Justin Gilmer, Samuel S. Schoenholz, Patrick F. Riley, Oriol Vinyals, and George E. Dahl. Neural message passing for quantum chemistry. In Doina Precup and Yee Whye Teh, editors, *Proceedings of the 34th International Conference on Machine Learning*, volume 70 of *Proceedings of Machine Learning Research*, pages 1263–1272. PMLR, 06–11 Aug 2017.

[140] Solveig Klepper and Ulrike von Luxburg. Relating graph auto-encoders to linear models, November 2022. URL <http://arxiv.org/abs/2211.01858>. arXiv:2211.01858 [cs].

[141] Marc Brockschmidt. GNN-FiLM: Graph Neural Networks with Feature-wise Linear Modulation, June 2020. URL <http://arxiv.org/abs/1906.12192>. arXiv:1906.12192 [cs, stat].

[142] Felix Wu, Tianyi Zhang, Amauri Holanda de Souza Jr., Christopher Fifty, Tao Yu, and Kilian Q. Weinberger. Simplifying Graph Convolutional Networks. *arXiv:1902.07153 [cs, stat]*, June 2019. URL <http://arxiv.org/abs/1902.07153>. arXiv: 1902.07153.

[143] Ferran Alet, Adarsh Keshav Jeewajee, Maria Bauza Villalonga, Alberto Rodriguez, Tomas Lozano-Perez, and Leslie Kaelbling. Graph element networks: adaptive, structured computation and memory. In Kamalika Chaudhuri and Ruslan Salakhutdinov, editors, *Proceedings of the 36th International Conference on Machine Learning*, volume 97 of *Proceedings of Machine Learning Research*, pages 212–222. PMLR, 09–15 Jun 2019.

[144] Meire Fortunato, Tobias Pfaff, Peter Wirsberger, Alexander Pritzel, and Peter Battaglia. MultiScale MeshGraph-Nets, October 2022. URL <http://arxiv.org/abs/2210.00612>. arXiv:2210.00612 [cs].

[145] Tobias Pfaff, Meire Fortunato, Alvaro Sanchez-Gonzalez, and Peter Battaglia. Learning mesh-based simulation with graph networks. In *International Conference on Learning Representations*, 2021.

[146] Alvaro Sanchez-Gonzalez, Nicolas Heess, Jost Tobias Springenberg, Josh Merel, Martin Riedmiller, Raia Hadsell, and Peter Battaglia. Graph networks as learnable physics engines for inference and control. *arXiv:1806.01242 [cs, stat]*, June 2018. URL <http://arxiv.org/abs/1806.01242>. arXiv: 1806.01242.

[147] Salva Rühling Cachay, Emma Erickson, Arthur Fender C. Bucker, Ernest Pokropek, Willa Potosnak, Suyash Bire, Salomey Osei, and Björn Lütjens. The World as a Graph: Improving El Niño Forecasts with Graph Neural Networks. *arXiv:2104.05089 [physics, stat]*, May 2021. URL <http://arxiv.org/abs/2104.05089>. arXiv: 2104.05089.

[148] Jean-Baptiste Cordonnier, Andreas Loukas, and Martin Jaggi. On the relationship between self-attention and convolutional layers. In *International Conference on Learning Representations*, 2020.

[149] Chaoqi Chen, Yushuang Wu, Qiyuan Dai, Hong-Yu Zhou, Mutian Xu, Sibei Yang, Xiaoguang Han, and Yizhou Yu. A Survey on Graph Neural Networks and Graph Transformers in Computer Vision: A Task-Oriented Perspective, October 2022. URL <http://arxiv.org/abs/2209.13232>. arXiv:2209.13232 [cs].

[150] Peter Shaw, Jakob Uszkoreit, and Ashish Vaswani. Self-attention with relative position representations. In *Proceedings of the 2018 Conference of the North American Chapter of the Association for Computational Linguistics: Human Language Technologies, Volume 2 (Short Papers)*, pages 464–468, New Orleans, Louisiana, June 2018. Association for Computational Linguistics. doi:10.18653/v1/N18-2074.

[151] Yao-Hung Hubert Tsai, Shaojie Bai, Makoto Yamada, Louis-Philippe Morency, and Ruslan Salakhutdinov. Transformer dissection: An unified understanding for transformer’s attention via the lens of kernel. In *Proceedings of the 2019 Conference on Empirical Methods in Natural Language Processing and the 9th International Joint Conference on Natural Language Processing (EMNLP-IJCNLP)*, pages 4344–4353, Hong Kong, China, November 2019. Association for Computational Linguistics. doi:10.18653/v1/D19-1443.

[152] Pierre Baldi and Roman Vershynin. The Quarks of Attention. *arXiv:2202.08371 [cs, stat]*, February 2022. URL <http://arxiv.org/abs/2202.08371>. arXiv: 2202.08371.

[153] Gedas Bertasius, Heng Wang, and Lorenzo Torresani. Is space-time attention all you need for video understanding? In Marina Meila and Tong Zhang, editors, *Proceedings of the 38th International Conference on Machine Learning*, volume 139 of *Proceedings of Machine Learning Research*, pages 813–824. PMLR, 18–24 Jul 2021.

[154] Zonghan Wu, Shirui Pan, Guodong Long, Jing Jiang, Xiaojun Chang, and Chengqi Zhang. Connecting the dots: Multivariate time series forecasting with graph neural networks. In *Proceedings of the 26th ACM SIGKDD International Conference on Knowledge Discovery & Data Mining*, pages 753–763, New York, NY, USA, 2020. Association for Computing Machinery. ISBN 9781450379984. doi:10.1145/3394486.3403118.

[155] Konstantin Klemmer, Nathan Safir, and Daniel B Neill. Positional encoder graph neural networks for geographic data. In *Proceedings of The 26th International Conference on Artificial Intelligence and Statistics*, Proceedings of Machine Learning Research. PMLR, 2023.

[156] Kan Wu, Houwen Peng, Minghao Chen, Jianlong Fu, and Hongyang Chao. Rethinking and Improving Relative Position Encoding for Vision Transformer. In *2021 IEEE/CVF International Conference on Computer Vision (ICCV)*, pages 10013–10021, Montreal, QC, Canada, October 2021. IEEE. ISBN 978-1-66542-812-5. doi:10.1109/ICCV48922.2021.00988. URL <https://ieeexplore.ieee.org/document/9710917/>.

[157] Md Amirul Islam, Sen Jia, and Neil D. B. Bruce. How much position information do convolutional neural networks encode? In *International Conference on Learning Representations*, 2020.

[158] Thomas N. Kipf and Max Welling. Semi-supervised classification with graph convolutional networks. In *International Conference on Learning Representations*, 2017.

[159] Kaiming He, Xiangyu Zhang, Shaoqing Ren, and Jian Sun. Delving Deep into Rectifiers: Surpassing Human-Level Performance on ImageNet Classification. In *2015 IEEE International Conference on Computer Vision (ICCV)*, pages 1026–1034, Santiago, Chile, December 2015. IEEE. ISBN 978-1-4673-8391-2. doi:[10.1109/ICCV.2015.123](https://doi.org/10.1109/ICCV.2015.123). URL <http://ieeexplore.ieee.org/document/7410480/>.

[160] Kaiming He, Xiangyu Zhang, Shaoqing Ren, and Jian Sun. Deep residual learning for image recognition. In *2016 IEEE Conference on Computer Vision and Pattern Recognition (CVPR)*, pages 770–778, 2016. doi:[10.1109/CVPR.2016.90](https://doi.org/10.1109/CVPR.2016.90).

[161] Sergey Ioffe and Christian Szegedy. Batch normalization: Accelerating deep network training by reducing internal covariate shift. In *Proceedings of the 32nd International Conference on International Conference on Machine Learning - Volume 37*, ICML’15, page 448–456. JMLR.org, 2015.

[162] Jimmy Lei Ba, Jamie Ryan Kiros, and Geoffrey E. Hinton. Layer Normalization. *arXiv:1607.06450 [cs, stat]*, July 2016. URL <http://arxiv.org/abs/1607.06450>. arXiv: 1607.06450.

[163] Yuxin Wu and Kaiming He. Group Normalization. *International Journal of Computer Vision*, 128(3):742–755, March 2020. ISSN 0920-5691, 1573-1405. doi:[10.1007/s11263-019-01198-w](https://doi.org/10.1007/s11263-019-01198-w).

[164] Dmitry Ulyanov, Andrea Vedaldi, and Victor Lempitsky. Instance Normalization: The Missing Ingredient for Fast Stylization, November 2017. URL <http://arxiv.org/abs/1607.08022>. arXiv:1607.08022 [cs].

[165] Takeru Miyato, Toshiki Kataoka, Masanori Koyama, and Yuichi Yoshida. Spectral normalization for generative adversarial networks. In *International Conference on Learning Representations*, 2018.

[166] H. Touvron, M. Cord, A. Sablayrolles, G. Synnaeve, and H. Jegou. Going deeper with image transformers. In *2021 IEEE/CVF International Conference on Computer Vision (ICCV)*, pages 32–42, Los Alamitos, CA, USA, oct 2021. IEEE Computer Society. doi:[10.1109/ICCV48922.2021.00010](https://doi.org/10.1109/ICCV48922.2021.00010).

[167] Shibani Santurkar, Dimitris Tsipras, Andrew Ilyas, and Aleksander Madry. How does batch normalization help optimization? In S. Bengio, H. Wallach, H. Larochelle, K. Grauman, N. Cesa-Bianchi, and R. Garnett, editors, *Advances in Neural Information Processing Systems*, volume 31. Curran Associates, Inc., 2018.

[168] Andrew Brock, Soham De, and Samuel L Smith. Characterizing signal propagation to close the performance gap in unnormalized resnets. In *International Conference on Learning Representations*, 2021.

[169] Andrew Brock, Soham De, Samuel L. Smith, and Karen Simonyan. High-Performance Large-Scale Image Recognition Without Normalization. *arXiv:2102.06171 [cs, stat]*, February 2021. URL <http://arxiv.org/abs/2102.06171>. arXiv: 2102.06171.

[170] Xun Huang and Serge Belongie. Arbitrary style transfer in real-time with adaptive instance normalization. In *2017 IEEE International Conference on Computer Vision (ICCV)*, pages 1510–1519, 2017. doi:[10.1109/ICCV.2017.167](https://doi.org/10.1109/ICCV.2017.167).

[171] Ethan Perez, Florian Strub, Harm de Vries, Vincent Dumoulin, and Aaron Courville. Film: Visual reasoning with a general conditioning layer. In *AAAI’18/IAAI’18/EAAI’18*. AAAI Press, 2018. ISBN 978-1-57735-800-8.

[172] Peter L. Bartlett, Andrea Montanari, and Alexander Rakhlin. Deep learning: a statistical viewpoint. *Acta Numerica*, 30:87–201, May 2021. ISSN 0962-4929, 1474-0508. doi:[10.1017/S0962492921000027](https://doi.org/10.1017/S0962492921000027). URL [https://www.cambridge.org/core/product/identifier/S0962492921000027/type/journal\\_article](https://www.cambridge.org/core/product/identifier/S0962492921000027/type/journal_article).

[173] Herbert Robbins and Sutton Monro. A Stochastic Approximation Method. *The Annals of Mathematical Statistics*, 22(3):400–407, September 1951. ISSN 0003-4851, 2168-8990. doi:[10.1214/aoms/1177729586](https://doi.org/10.1214/aoms/1177729586). URL <https://projecteuclid.org/journals/annals-of-mathematical-statistics/volume-22/issue-3/A-Stochastic-Approximation-Method/10.1214/aoms/1177729586.full>. Publisher: Institute of Mathematical Statistics.

[174] Léon Bottou. On-line Learning and Stochastic Approximations. In *On-Line Learning in Neural Networks*, pages 9–42. Cambridge University Press, 1 edition, January 1999. ISBN 978-0-521-65263-6 978-0-521-11791-3 978-0-511-56992-0. doi:[10.1017/CBO9780511569920.003](https://doi.org/10.1017/CBO9780511569920.003). URL [https://www.cambridge.org/core/product/identifier/CBO9780511569920A009/type/book\\_part](https://www.cambridge.org/core/product/identifier/CBO9780511569920A009/type/book_part).

[175] Chen Xing, Devansh Arpit, Christos Tsirigotis, and Yoshua Bengio. A Walk with SGD. *arXiv:1802.08770 [cs, stat]*, May 2018. URL <http://arxiv.org/abs/1802.08770>. arXiv: 1802.08770.

[176] Sepp Hochreiter and Jürgen Schmidhuber. Flat Minima. *Neural Computation*, 9(1):1–42, January 1997. ISSN 0899-7667. doi:[10.1162/neco.1997.9.1.1](https://doi.org/10.1162/neco.1997.9.1.1). URL <https://doi.org/10.1162/neco.1997.9.1.1>.

[177] Nitish Shirish Keskar, Dheevatsa Mudigere, Jorge Nocedal, Mikhail Smelyanskiy, and Ping Tak Peter Tang. On large-batch training for deep learning: Generalization gap and sharp minima. In *International Conference on Learning Representations*, 2017.

[178] Vladimir N. Vapnik. *The Nature of Statistical Learning Theory*. Springer, New York, NY, 2000. ISBN 978-1-4419-3160-3 978-1-4757-3264-1. doi:10.1007/978-1-4757-3264-1. URL <http://link.springer.com/10.1007/978-1-4757-3264-1>.

[179] Tom Brown, Benjamin Mann, Nick Ryder, Melanie Subbiah, Jared D Kaplan, Prafulla Dhariwal, Arvind Neelakantan, Pranav Shyam, Girish Sastry, Amanda Askell, Sandhini Agarwal, Ariel Herbert-Voss, Gretchen Krueger, Tom Henighan, Rewon Child, Aditya Ramesh, Daniel Ziegler, Jeffrey Wu, Clemens Winter, Chris Hesse, Mark Chen, Eric Sigler, Mateusz Litwin, Scott Gray, Benjamin Chess, Jack Clark, Christopher Berner, Sam McCandlish, Alec Radford, Ilya Sutskever, and Dario Amodei. Language models are few-shot learners. In H. Larochelle, M. Ranzato, R. Hadsell, M.F. Balcan, and H. Lin, editors, *Advances in Neural Information Processing Systems*, volume 33, pages 1877–1901. Curran Associates, Inc., 2020. URL [https://proceedings.neurips.cc/paper\\_files/paper/2020/file/1457c0d6bfc4967418bfb8ac142f64a-Paper.pdf](https://proceedings.neurips.cc/paper_files/paper/2020/file/1457c0d6bfc4967418bfb8ac142f64a-Paper.pdf).

[180] Mikhail Belkin, Daniel Hsu, Siyuan Ma, and Soumik Mandal. Reconciling modern machine learning practice and the bias-variance trade-off. *Proceedings of the National Academy of Sciences*, 116(32):15849–15854, August 2019. ISSN 0027-8424, 1091-6490. doi:10.1073/pnas.1903070116. URL <http://arxiv.org/abs/1812.11118>. arXiv:1812.11118 [cs, stat].

[181] Mikhail Belkin. Fit without fear: remarkable mathematical phenomena of deep learning through the prism of interpolation. *Acta Numerica*, 30:203–248, 2021. doi:10.1017/S0962492921000039.

[182] Jared Kaplan, Sam McCandlish, Tom Henighan, Tom B. Brown, Benjamin Chess, Rewon Child, Scott Gray, Alec Radford, Jeffrey Wu, and Dario Amodei. Scaling Laws for Neural Language Models, January 2020. URL <http://arxiv.org/abs/2001.08361>. arXiv:2001.08361 [cs, stat].

[183] Jordan Hoffmann, Sebastian Borgeaud, Arthur Mensch, Elena Buchatskaya, Trevor Cai, Eliza Rutherford, Diego de Las Casas, Lisa Anne Hendricks, Johannes Welbl, Aidan Clark, et al. Training compute-optimal large language models. *arXiv preprint arXiv:2203.15556*, 2022.

[184] Alexander Maloney, Daniel A. Roberts, and James Sully. A Solvable Model of Neural Scaling Laws, October 2022. URL <http://arxiv.org/abs/2210.16859>. arXiv:2210.16859 [hep-th, stat].

[185] Priya Goyal, Piotr Dollár, Ross Girshick, Pieter Noordhuis, Lukasz Wesolowski, Aapo Kyrola, Andrew Tulloch, Yangqing Jia, and Kaiming He. Accurate, Large Minibatch SGD: Training ImageNet in 1 Hour, April 2018. URL <http://arxiv.org/abs/1706.02677>. Number: arXiv:1706.02677 arXiv:1706.02677 [cs].

[186] Samuel L. Smith, Pieter-Jan Kindermans, Chris Ying, and Quoc V. Le. Don’t Decay the Learning Rate, Increase the Batch Size. *arXiv:1711.00489 [cs, stat]*, February 2018. URL <http://arxiv.org/abs/1711.00489>. arXiv: 1711.00489.

[187] Diederik P. Kingma and Jimmy Ba. Adam: A Method for Stochastic Optimization. In *International Conference on Learning Representations*, 2015.

[188] Ilya Loshchilov and Frank Hutter. Decoupled weight decay regularization. In *International Conference on Learning Representations*, 2019.

[189] Ilya Sutskever, James Martens, George Dahl, and Geoffrey Hinton. On the importance of initialization and momentum in deep learning. In *Proceedings of the 30th International Conference on International Conference on Machine Learning - Volume 28*, ICML’13, page III–1139–III–1147. JMLR.org, 2013.

[190] Ilya Loshchilov and Frank Hutter. SGDR: Stochastic gradient descent with warm restarts. In *International Conference on Learning Representations*, 2017.

[191] Leslie N. Smith and Nicholay Topin. Super-convergence: very fast training of neural networks using large learning rates. In *Artificial Intelligence and Machine Learning for Multi-Domain Operations Applications*, volume 11006, page 1100612. International Society for Optics and Photonics, SPIE, 2019. doi:10.1117/12.2520589.

[192] Leslie N. Smith. Cyclical Learning Rates for Training Neural Networks. *arXiv:1506.01186 [cs]*, April 2017. URL <http://arxiv.org/abs/1506.01186>. arXiv: 1506.01186.

[193] Yoshua Bengio, Jérôme Louradour, Ronan Collobert, and Jason Weston. Curriculum learning. In *Proceedings of the 26th Annual International Conference on Machine Learning*, ICML ’09, pages 41–48, New York, NY, USA, June 2009. Association for Computing Machinery. ISBN 978-1-60558-516-1. doi:10.1145/1553374.1553380. URL <https://doi.org/10.1145/1553374.1553380>.

[194] Jacob Devlin, Ming-Wei Chang, Kenton Lee, and Kristina Toutanova. BERT: Pre-training of deep bidirectional transformers for language understanding. In *Proceedings of the 2019 Conference of the North American Chapter of the Association for Computational Linguistics: Human Language Technologies, Volume 1 (Long and Short Papers)*, pages 4171–4186, Minneapolis, Minnesota, June 2019. Association for Computational Linguistics. doi:[10.18653/v1/N19-1423](https://doi.org/10.18653/v1/N19-1423).

[195] Kaiming He, Xinlei Chen, Saining Xie, Yanghao Li, Piotr Dollár, and Ross Girshick. Masked Autoencoders Are Scalable Vision Learners, December 2021. URL <http://arxiv.org/abs/2111.06377>. arXiv:2111.06377 [cs].

[196] Yoshua Bengio, Pascal Lamblin, Dan Popovici, and Hugo Larochelle. Greedy layer-wise training of deep networks. In *Advances in Neural Information Processing Systems*, volume 19. MIT Press, 2006.

[197] Dumitru Erhan, Pierre-Antoine Manzagol, Yoshua Bengio, Samy Bengio, and Pascal Vincent. The Difficulty of Training Deep Architectures and the Effect of Unsupervised Pre-Training. In *Proceedings of the Twelfth International Conference on Artificial Intelligence and Statistics*, pages 153–160. PMLR, April 2009. URL <https://proceedings.mlr.press/v5/erhan09a.html>.

[198] Nitish Srivastava, Geoffrey Hinton, Alex Krizhevsky, Ilya Sutskever, and Ruslan Salakhutdinov. Dropout: A simple way to prevent neural networks from overfitting. *Journal of Machine Learning Research*, 15(56):1929–1958, 2014.

[199] Golnaz Ghiasi, Tsung-Yi Lin, and Quoc V Le. Dropblock: A regularization method for convolutional networks. In S. Bengio, H. Wallach, H. Larochelle, K. Grauman, N. Cesa-Bianchi, and R. Garnett, editors, *Advances in Neural Information Processing Systems*, volume 31. Curran Associates, Inc., 2018.

[200] Zuxuan Wu, Tushar Nagarajan, Abhishek Kumar, Steven Rennie, Larry S. Davis, Kristen Grauman, and Rogério Schmidt Feris. Blockdrop: Dynamic inference paths in residual networks. In *2018 IEEE Conference on Computer Vision and Pattern Recognition, CVPR 2018, Salt Lake City, UT, USA, June 18-22, 2018*, pages 8817–8826. Computer Vision Foundation / IEEE Computer Society, 2018. doi:[10.1109/CVPR.2018.00919](https://doi.org/10.1109/CVPR.2018.00919).

[201] Gustav Larsson, Michael Maire, and Gregory Shakhnarovich. Fractalnet: Ultra-deep neural networks without residuals. In *International Conference on Learning Representations*, 2017.

[202] Akhilesh Gotmare, Nitish Shirish Keskar, Caiming Xiong, and Richard Socher. Using Mode Connectivity for Loss Landscape Analysis. *arXiv:1806.06977 [cs, stat]*, June 2018. URL <http://arxiv.org/abs/1806.06977>. arXiv: 1806.06977.

[203] Akhilesh Gotmare, Nitish Shirish Keskar, Caiming Xiong, and Richard Socher. A closer look at deep learning heuristics: Learning rate restarts, warmup and distillation. In *International Conference on Learning Representations*, 2019.

[204] Timur Garipov, Pavel Izmailov, Dmitrii Podoprikhin, Dmitry Vetrov, and Andrew Gordon Wilson. Loss surfaces, mode connectivity, and fast ensembling of dnns. In *Proceedings of the 32nd International Conference on Neural Information Processing Systems*, NIPS’18, pages 8803–8812, Red Hook, NY, USA, 2018. Curran Associates Inc.

[205] Matthew Chantry, Hannah Christensen, Peter Dueben, and Tim Palmer. Opportunities and challenges for machine learning in weather and climate modelling: hard, medium and soft AI. *Philosophical Transactions of the Royal Society A: Mathematical, Physical and Engineering Sciences*, 379(2194):20200083, April 2021. doi:[10.1098/rsta.2020.0083](https://doi.org/10.1098/rsta.2020.0083). URL <https://royalsocietypublishing.org/doi/10.1098/rsta.2020.0083>. Publisher: Royal Society.

[206] M. G. Schultz, C. Betancourt, B. Gong, F. Kleinert, M. Langguth, L. H. Leufen, A. Mozaffari, and S. Stadtler. Can deep learning beat numerical weather prediction? *Philosophical Transactions of the Royal Society A: Mathematical, Physical and Engineering Sciences*, 379(2194):20200097, April 2021. doi:[10.1098/rsta.2020.0097](https://doi.org/10.1098/rsta.2020.0097). URL <https://royalsocietypublishing.org/doi/full/10.1098/rsta.2020.0097>. Publisher: Royal Society.

[207] Anuj Karpatne, Gowtham Atluri, James H. Faghmous, Michael Steinbach, Arindam Banerjee, Auroop Ganguly, Shashi Shekhar, Nagiza Samatova, and Vipin Kumar. Theory-Guided Data Science: A New Paradigm for Scientific Discovery from Data. *IEEE Transactions on Knowledge and Data Engineering*, 29(10):2318–2331, October 2017. ISSN 1558-2191. doi:[10.1109/TKDE.2017.2720168](https://doi.org/10.1109/TKDE.2017.2720168). Conference Name: IEEE Transactions on Knowledge and Data Engineering.

[208] Anuj Karpatne, Imme Ebert-Uphoff, Sai Ravela, Hassan Ali Babaie, and Vipin Kumar. Machine Learning for the Geosciences: Challenges and Opportunities. *IEEE Transactions on Knowledge and Data Engineering*, 31(8):1544–1554, August 2019. ISSN 1558-2191. doi:[10.1109/TKDE.2018.2861006](https://doi.org/10.1109/TKDE.2018.2861006). Conference Name: IEEE Transactions on Knowledge and Data Engineering.

[209] George Em Karniadakis, Ioannis G. Kevrekidis, Lu Lu, Paris Perdikaris, Sifan Wang, and Liu Yang. Physics-informed machine learning. *Nature Reviews Physics*, 3(6):422–440, June 2021. ISSN 2522-5820. doi:[10.1038/s42254-021-00314-5](https://doi.org/10.1038/s42254-021-00314-5). URL <https://www.nature.com/articles/s42254-021-00314-5>. Number: 6 Publisher: Nature Publishing Group.

[210] Chuizheng Meng, Sungyong Seo, Defu Cao, Sam Griesemer, and Yan Liu. When Physics Meets Machine Learning: A Survey of Physics-Informed Machine Learning, March 2022. URL <http://arxiv.org/abs/2203.16797>. arXiv:2203.16797 [cs, stat].

[211] Nils Thuerey, Philipp Holl, Maximilian Mueller, Patrick Schnell, Felix Trost, and Kiwon Um. Physics-based Deep Learning, April 2022. URL <http://arxiv.org/abs/2109.05237>. arXiv:2109.05237 [physics].

[212] Tom Beucler, Michael Pritchard, Pierre Gentine, and Stephan Rasp. Towards physically-consistent, data-driven models of convection. In *IGARSS 2020 - 2020 IEEE International Geoscience and Remote Sensing Symposium*, pages 3987–3990, 2020. doi:[10.1109/IGARSS39084.2020.9324569](https://doi.org/10.1109/IGARSS39084.2020.9324569).

[213] Tom Beucler, Michael Pritchard, Stephan Rasp, Jordan Ott, Pierre Baldi, and Pierre Gentine. Enforcing Analytic Constraints in Neural-Networks Emulating Physical Systems. *Physical Review Letters*, 126(9):098302, March 2021. ISSN 0031-9007, 1079-7114. doi:[10.1103/PhysRevLett.126.098302](https://doi.org/10.1103/PhysRevLett.126.098302). URL <http://arxiv.org/abs/1909.00912>. arXiv:1909.00912 [physics].

[214] Tom Beucler, Stephan Rasp, Michael Pritchard, and Pierre Gentine. Achieving Conservation of Energy in Neural Network Emulators for Climate Modeling. *arXiv:1906.06622 [physics]*, June 2019. URL <http://arxiv.org/abs/1906.06622>. arXiv: 1906.06622.

[215] Yu Huang, Yufei Tang, Hanqi Zhuang, James VanZwieten, and Laurent Cherubin. Physics-informed Tensor-train ConvLSTM for Volumetric Velocity Forecasting of Loop Current. *Frontiers in Artificial Intelligence*, 4:780271, December 2021. ISSN 2624-8212. doi:[10.3389/frai.2021.780271](https://doi.org/10.3389/frai.2021.780271). URL <http://arxiv.org/abs/2008.01798>. arXiv:2008.01798 [cs, eess, stat].

[216] M. Raissi, P. Perdikaris, and G.E. Karniadakis. Physics-informed neural networks: A deep learning framework for solving forward and inverse problems involving nonlinear partial differential equations. *Journal of Computational Physics*, 378:686–707, 2019. ISSN 0021-9991. doi:<https://doi.org/10.1016/j.jcp.2018.10.045>. URL <https://www.sciencedirect.com/science/article/pii/S0021999118307125>.

[217] M. Raissi, P. Perdikaris, and G.E. Karniadakis. Physics-informed neural networks: A deep learning framework for solving forward and inverse problems involving nonlinear partial differential equations. *Journal of Computational Physics*, 378:686–707, 2019. ISSN 0021-9991. doi:<https://doi.org/10.1016/j.jcp.2018.10.045>.

[218] Matthias Karlbauer, Timothy Praditia, Sebastian Otte, Sergey Oladyshkin, Wolfgang Nowak, and Martin V. Butz. Composing partial differential equations with physics-aware neural networks. In Kamalika Chaudhuri, Stefanie Jegelka, Le Song, Csaba Szepesvari, Gang Niu, and Sivan Sabato, editors, *Proceedings of the 39th International Conference on Machine Learning*, volume 162 of *Proceedings of Machine Learning Research*, pages 10773–10801. PMLR, 17–23 Jul 2022.

[219] Timothy Praditia, Matthias Karlbauer, Sebastian Otte, Sergey Oladyshkin, Martin V. Butz, and Wolfgang Nowak. Learning Groundwater Contaminant Diffusion-Sorption Processes With a Finite Volume Neural Network. *Water Resources Research*, 58(12):e2022WR033149, 2022. ISSN 1944-7973. doi:[10.1029/2022WR033149](https://doi.org/10.1029/2022WR033149). URL <https://onlinelibrary.wiley.com/doi/abs/10.1029/2022WR033149>.

[220] Salvatore Cuomo, Vincenzo Schiano Di Cola, Fabio Giampaolo, Gianluigi Rozza, Maziar Raissi, and Francesco Piccialli. Scientific machine learning through physics-informed neural networks: Where we are and what’s next. *Journal of Scientific Computing*, 92(3):88, 2022. doi:[10.1007/s10915-022-01939-z](https://doi.org/10.1007/s10915-022-01939-z). URL <https://doi.org/10.1007/s10915-022-01939-z>.

[221] Zongyi Li, Hongkai Zheng, Nikola Kovachki, David Jin, Haoxuan Chen, Burigede Liu, Kamyr Azizzadenesheli, and Anima Anandkumar. Physics-Informed Neural Operator for Learning Partial Differential Equations, November 2021. URL <http://arxiv.org/abs/2111.03794>. Number: arXiv:2111.03794 arXiv:2111.03794 [cs, math].

[222] T. N. Palmer, G. J. Shutts, R. Hagedorn, F. J. Doblas-Reyes, T. Jung, and M. Leutbecher. Representing Model Uncertainty in Weather and Climate Prediction. *Annual Review of Earth and Planetary Sciences*, 33:163–193, January 2005. ISSN 0084-6597. doi:[10.1146/annurev.earth.33.092203.122552](https://doi.org/10.1146/annurev.earth.33.092203.122552). URL <https://ui.adsabs.harvard.edu/abs/2005AREPS..33..163P>. ADS Bibcode: 2005AREPS..33..163P.

[223] Roberto Buizza, M Milleer, and Tim N Palmer. Stochastic representation of model uncertainties in the ECMWF ensemble prediction system. *Quarterly Journal of the Royal Meteorological Society*, 125(560):2887–2908, 1999. Publisher: Wiley Online Library.

[224] T.N. Palmer, Roberto Buizza, F. Doblas-Reyes, T. Jung, Martin Leutbecher, G.J. Shutts, M. Steinheimer, and Antje Weisheimer. Stochastic parametrization and model uncertainty. *ECMWF Technical Memoranda*, page 42, 10/2009 2009. doi:[10.21957/ps8gbwbdv](https://doi.org/10.21957/ps8gbwbdv).

[225] Peter D. Düben, Hugh McNamara, and T. N. Palmer. The use of imprecise processing to improve accuracy in weather & climate prediction. *Journal of Computational Physics*, 271:2–18, August 2014. ISSN 0021-9991. doi:[10.1016/j.jcp.2013.10.042](https://doi.org/10.1016/j.jcp.2013.10.042). URL <https://www.sciencedirect.com/science/article/pii/S0021999113007183>.

[226] Tobias Thornes, Peter Düben, and Tim Palmer. On the use of scale-dependent precision in Earth System modelling. *Quarterly Journal of the Royal Meteorological Society*, 143(703):897–908, 2017. ISSN 1477-870X. doi:[10.1002/qj.2974](https://doi.org/10.1002/qj.2974). URL <https://onlinelibrary.wiley.com/doi/abs/10.1002/qj.2974>.

[227] Filip Váňa, Peter Düben, Simon Lang, Tim Palmer, Martin Leutbecher, Deborah Salmond, and Glenn Carver. Single Precision in Weather Forecasting Models: An Evaluation with the IFS. *Monthly Weather Review*, 145(2):495–502, February 2017. ISSN 1520-0493, 0027-0644. doi:[10.1175/MWR-D-16-0228.1](https://doi.org/10.1175/MWR-D-16-0228.1). URL <https://journals.ametsoc.org/view/journals/mwre/145/2/mwr-d-16-0228.1.xml>. Publisher: American Meteorological Society Section: Monthly Weather Review.

[228] Tim Palmer. The primacy of doubt: Evolution of numerical weather prediction from determinism to probability. *Journal of Advances in Modeling Earth Systems*, 9(2):730–734, 2017. ISSN 1942-2466. doi:[10.1002/2017MS000999](https://doi.org/10.1002/2017MS000999).

[229] Tim Palmer and David Richardson. Decisions, decisions...! *ECMWF Newsletter*, pages 12–14, 2014 2014. doi:[10.21957/bychj3cf](https://doi.org/10.21957/bychj3cf).

[230] T. N. Palmer. A personal perspective on modelling the climate system. *Proceedings of the Royal Society A: Mathematical, Physical and Engineering Sciences*, 472(2188):20150772, April 2016. doi:[10.1098/rspa.2015.0772](https://doi.org/10.1098/rspa.2015.0772). URL <https://royalsocietypublishing.org/doi/full/10.1098/rspa.2015.0772>. Publisher: Royal Society.

[231] R. Buizza and T. N. Palmer. The Singular-Vector Structure of the Atmospheric Global Circulation. *Journal of the Atmospheric Sciences*, 52(9):1434–1456, May 1995. ISSN 0022-4928, 1520-0469. doi:[10.1175/1520-0469\(1995\)052<1434:TSVSOT>2.0.CO;2](https://doi.org/10.1175/1520-0469(1995)052<1434:TSVSOT>2.0.CO;2). URL [https://journals.ametsoc.org/view/journals/atsc/52/9/1520-0469\\_1995\\_052\\_1434\\_tsvsot\\_2\\_0\\_co\\_2.xml](https://journals.ametsoc.org/view/journals/atsc/52/9/1520-0469_1995_052_1434_tsvsot_2_0_co_2.xml). Publisher: American Meteorological Society Section: Journal of the Atmospheric Sciences.

[232] T. N. Palmer, R. Gelaro, J. Barkmeijer, and R. Buizza. Singular Vectors, Metrics, and Adaptive Observations. *Journal of the Atmospheric Sciences*, 55(4):633–653, February 1998. ISSN 0022-4928, 1520-0469. doi:[10.1175/1520-0469\(1998\)055<0633:SVMAAO>2.0.CO;2](https://doi.org/10.1175/1520-0469(1998)055<0633:SVMAAO>2.0.CO;2). URL [https://journals.ametsoc.org/view/journals/atsc/55/4/1520-0469\\_1998\\_055\\_0633\\_svmaao\\_2.0.co\\_2.xml](https://journals.ametsoc.org/view/journals/atsc/55/4/1520-0469_1998_055_0633_svmaao_2.0.co_2.xml). Publisher: American Meteorological Society Section: Journal of the Atmospheric Sciences.

[233] National Academies of Sciences, Engineering, and Medicine. *Next Generation Earth System Prediction: Strategies for Subseasonal to Seasonal Forecasts*. The National Academies Press, Washington, DC, 2016. ISBN 978-0-309-38880-1. doi:[10.17226/21873](https://doi.org/10.17226/21873).

[234] E. A. Baggett, E. K.-M. Barnes, A. Chang, P. A. Lang, K. Dirmeyer, D. Piegion, C. Barrie, and A. Mariotti. Bridging the Weather-to-Climate Prediction Gap, February 2019. URL <http://eos.org/science-updates/bridging-the-weather-to-climate-prediction-gap>.

[235] F. Vitart, C. Ardilouze, A. Bonet, A. Brookshaw, M. Chen, C. Codorean, M. Déqué, L. Ferranti, E. Fucile, M. Fuentes, H. Hendon, J. Hodgson, H.-S. Kang, A. Kumar, H. Lin, G. Liu, X. Liu, P. Malguzzi, I. Mallas, M. Manoussakis, D. Mastrangelo, C. MacLachlan, P. McLean, A. Minami, R. Mladek, T. Nakazawa, S. Najm, Y. Nie, M. Rixen, A. W. Robertson, P. Ruti, C. Sun, Y. Takaya, M. Tolstykh, F. Venuti, D. Waliser, S. Woolnough, T. Wu, D.-J. Won, H. Xiao, R. Zaripov, and L. Zhang. The Subseasonal to Seasonal (S2S) Prediction Project Database. *Bulletin of the American Meteorological Society*, 98(1):163–173, January 2017. ISSN 0003-0007, 1520-0477. doi:[10.1175/BAMS-D-16-0017.1](https://doi.org/10.1175/BAMS-D-16-0017.1). URL <https://journals.ametsoc.org/view/journals/bams/98/1/bams-d-16-0017.1.xml>.

[236] F. Vitart, A. W. Robertson, A. Spring, F. Pinault, R. Roškar, W. Cao, S. Bech, A. Bienkowski, N. Caltabiano, E. De Coning, B. Denis, A. Dirkson, J. Dramsch, P. Dueben, J. Gierschendorf, H. S. Kim, K. Nowak, D. Landry, L. Lledó, L. Palma, S. Rasp, and S. Zhou. Outcomes of the WMO Prize Challenge to Improve Subseasonal to Seasonal Predictions Using Artificial Intelligence. *Bulletin of the American Meteorological Society*, 103(12):E2878–E2886, December 2022. ISSN 0003-0007, 1520-0477. doi:[10.1175/BAMS-D-22-0046.1](https://doi.org/10.1175/BAMS-D-22-0046.1). URL <https://journals.ametsoc.org/view/journals/bams/103/12/BAMS-D-22-0046.1.xml>. Publisher: American Meteorological Society Section: Bulletin of the American Meteorological Society.

[237] Ashesh Chattopadhyay, Ebrahim Nabizadeh, and Pedram Hassanzadeh. Analog Forecasting of Extreme-Causing Weather Patterns Using Deep Learning. *Journal of Advances in Modeling Earth Systems*, 12(2):e2019MS001958, 2020. ISSN 1942-2466. doi:[10.1029/2019MS001958](https://doi.org/10.1029/2019MS001958). URL <https://onlinelibrary.wiley.com/doi/abs/10.1029/2019MS001958>.

[238] Frédéric Vitart. Madden-Julian Oscillation prediction and teleconnections in the S2S database. *Quarterly Journal of the Royal Meteorological Society*, 143(706):2210–2220, 2017. ISSN 1477-870X. doi:[10.1002/qj.3079](https://doi.org/10.1002/qj.3079). URL <https://onlinelibrary.wiley.com/doi/abs/10.1002/qj.3079>.

[239] Niklas Boers, Bedartha Goswami, Aljoscha Rheinwalt, Bodo Bookhagen, Brian Hoskins, and Jürgen Kurths. Complex networks reveal global pattern of extreme-rainfall teleconnections. *Nature*, 566(7744):373–377, February 2019. ISSN 1476-4687. doi:[10.1038/s41586-018-0872-x](https://doi.org/10.1038/s41586-018-0872-x). URL <https://www.nature.com/articles/s41586-018-0872-x>.

[240] Annarita Mariotti, Cory Baggett, Elizabeth A. Barnes, Emily Becker, Amy Butler, Dan C. Collins, Paul A. Dirmeyer, Laura Ferranti, Nathaniel C. Johnson, Jeanine Jones, Ben P. Kirtman, Andrea L. Lang, Andrea Molod, Matthew Newman, Andrew W. Robertson, Siegfried Schubert, Duane E. Waliser, and John Albers. Windows of Opportunity for Skillful Forecasts Subseasonal to Seasonal and Beyond. *Bulletin of the American Meteorological Society*, 101(5):E608–E625, May 2020. ISSN 0003-0007, 1520-0477. doi:[10.1175/BAMS-D-18-0326.1](https://doi.org/10.1175/BAMS-D-18-0326.1). URL <https://journals.ametsoc.org/view/journals/bams/101/5/bams-d-18-0326.1.xml>. Publisher: American Meteorological Society Section: Bulletin of the American Meteorological Society.

[241] Antoine Delaunay and Hannah M. Christensen. Interpretable Deep Learning for Probabilistic MJO Prediction. *Geophysical Research Letters*, 49(16):e2022GL098566, 2022. ISSN 1944-8007. doi:[10.1029/2022GL098566](https://doi.org/10.1029/2022GL098566). URL <https://onlinelibrary.wiley.com/doi/abs/10.1029/2022GL098566>.

[242] K. Hasselmann. Stochastic climate models Part I. Theory. *Tellus*, 28(6):473–485, 1976. ISSN 2153-3490. doi:[10.1111/j.2153-3490.1976.tb00696.x](https://doi.org/10.1111/j.2153-3490.1976.tb00696.x). URL <https://onlinelibrary.wiley.com/doi/abs/10.1111/j.2153-3490.1976.tb00696.x>.

[243] Veronika Eyring, Sandrine Bony, Gerald A. Meehl, Catherine A. Senior, Bjorn Stevens, Ronald J. Stouffer, and Karl E. Taylor. Overview of the Coupled Model Intercomparison Project Phase 6 (CMIP6) experimental design and organization. *Geoscientific Model Development*, 9(5):1937–1958, May 2016. ISSN 1991-959X. doi:[10.5194/gmd-9-1937-2016](https://doi.org/10.5194/gmd-9-1937-2016). URL <https://gmd.copernicus.org/articles/9/1937/2016/>. Publisher: Copernicus GmbH.

[244] S. Rasp. Coupled online learning as a way to tackle instabilities and biases in neural network parameterizations: general algorithms and lorenz 96 case study (v1.0). *Geoscientific Model Development*, 13(5):2185–2196, 2020. doi:[10.5194/gmd-13-2185-2020](https://doi.org/10.5194/gmd-13-2185-2020).

[245] D. Watson-Parris, Y. Rao, D. Olivié, Ø. Seland, P. Nowack, G. Camps-Valls, P. Stier, S. Bouabid, M. Dewey, E. Fons, J. Gonzalez, P. Harder, K. Jeggle, J. Lenhardt, P. Manshausen, M. Novitasari, L. Ricard, and C. Roesch. ClimateBench v1.0: A Benchmark for Data-Driven Climate Projections. *Journal of Advances in Modeling Earth Systems*, 14(10):e2021MS002954, 2022. ISSN 1942-2466. doi:[10.1029/2021MS002954](https://doi.org/10.1029/2021MS002954). URL <https://onlinelibrary.wiley.com/doi/abs/10.1029/2021MS002954>.

[246] Martina Stockhause and Michael Lautenschlager. CMIP6 Data Citation of Evolving Data. *Data Science Journal*, 16(0):30, June 2017. ISSN 1683-1470. doi:[10.5334/dsj-2017-030](https://doi.org/10.5334/dsj-2017-030). Number: 0 Publisher: Ubiquity Press.

[247] Rui Wang, Robin Walters, and Rose Yu. Meta-learning dynamics forecasting using task inference. In *Advances in Neural Information Processing Systems*, volume 35, pages 21640–21653. Curran Associates, Inc., 2022.

[248] Rishi Bommasani, Drew A. Hudson, Ehsan Adeli, Russ Altman, Simran Arora, Sydney von Arx, Michael S. Bernstein, Jeannette Bohg, Antoine Bosselut, Emma Brunskill, Erik Brynjolfsson, Shyamal Buch, Dallas Card, Rodrigo Castellon, Niladri Chatterji, Annie Chen, Kathleen Creel, Jared Quincy Davis, Dora Demszky, Chris Donahue, Moussa Doumbouya, Esin Durmus, Stefano Ermon, John Etchemendy, Kawin Ethayarajh, Li Fei-Fei, Chelsea Finn, Trevor Gale, Lauren Gillespie, Karan Goel, Noah Goodman, Shelby Grossman, Neel Guha, Tatsunori Hashimoto, Peter Henderson, John Hewitt, Daniel E. Ho, Jenny Hong, Kyle Hsu, Jing Huang, Thomas Icard, Saahil Jain, Dan Jurafsky, Pratyusha Kalluri, Siddharth Karamcheti, Geoff Keeling, Fereshte Khani, Omar Khattab, Pang Wei Koh, Mark Krass, Ranjay Krishna, Rohith Kuditipudi, Ananya Kumar, Faisal Ladhak, Mina Lee, Tony Lee, Jure Leskovec, Isabelle Levent, Xiang Lisa Li, Xuechen Li, Tengyu Ma, Ali Malik, Christopher D. Manning, Suvir Mirchandani, Eric Mitchell, Zanele Munyikwa, Suraj Nair, Avanika Narayan, Deepak Narayanan, Ben Newman, Allen Nie, Juan Carlos Niebles, Hamed Nilforoshan, Julian Nyarko, Giray O gut, Laurel Orr, Isabel Papadimitriou, Joon Sung Park, Chris Piech, Eva Portelance, Christopher Potts, Aditi Raghunathan, Rob Reich, Hongyu Ren, Frieda Rong, Yusuf Roohani, Camilo Ruiz, Jack Ryan, Christopher Ré, Dorsa Sadigh, Shiori Sagawa, Keshav Santhanam, Andy Shih, Krishnan Srinivasan, Alex Tamkin, Rohan Taori, Armin W.

Thomas, Florian Tramèr, Rose E. Wang, William Wang, Bohan Wu, Jiajun Wu, Yuhuai Wu, Sang Michael Xie, Michihiro Yasunaga, Jiaxuan You, Matei Zaharia, Michael Zhang, Tianyi Zhang, Xikun Zhang, Yuhui Zhang, Lucia Zheng, Kaitlyn Zhou, and Percy Liang. On the opportunities and risks of foundation models, 2022.

[249] Tung Nguyen, Johannes Brandstetter, Ashish Kapoor, Jayesh K. Gupta, and Aditya Grover. ClimaX: A foundation model for weather and climate, January 2023. URL <http://arxiv.org/abs/2301.10343>. arXiv:2301.10343 [cs].

[250] Mathilde Caron, Hugo Touvron, Ishan Misra, Hervé Jégou, Julien Mairal, Piotr Bojanowski, and Armand Joulin. Emerging properties in self-supervised vision transformers. In *Proceedings of the International Conference on Computer Vision (ICCV)*, 2021.

[251] Jeff Donahue and Karen Simonyan. Large scale adversarial representation learning. In *Proceedings of the 33rd International Conference on Neural Information Processing Systems*, Red Hook, NY, USA, 2019. Curran Associates Inc.

[252] Kaiming He, Haoqi Fan, Yuxin Wu, Saining Xie, and Ross Girshick. Momentum contrast for unsupervised visual representation learning. In *2020 IEEE/CVF Conference on Computer Vision and Pattern Recognition (CVPR)*, pages 9726–9735, 2020. doi:10.1109/CVPR42600.2020.00975.

[253] Yann LeCun. A Path Towards Autonomous Machine Intelligence. *OpenReview Archive*, 2022.